INITIALIZATION IN THE TROPICS

A. Hollingsworth and G. Cats
European Centre for Medium Range Weather Forecasts

1. THE PROBLEM

The non-linear normal mode initialization procedure (Temperton and Williamson 1979) has been in use at ECMWF for about two years. The main motivation for using the initialization is to control rapid oscillations in the short (6 hour) forecasts which are an essential part of the data assimilation. The medium range forecasts are also run from initialized data. The justification for this is not as strong as it is for the assimilation forecasts. The indications are that there is not much difference in medium range forecasts run from initialized and uninitialized data. However at the beginning of our operations it was not clear how sensitive the semi-implicit scheme would be to the use of uninitialized data (such data can easily have instantaneous initial pressure tendencies f 25 mb/3 hour), so that the decision to run from initialized data was taken for safety.

The mid-latitude vertical velocities in the initialized data are physically very reasonable and there are good theoretical reasons why this should be so (Leith 1980). However the initialization procedure has a strong effect on the tropical divergence fields.

The Centre's analysis scheme can analyse very convincing large scale divergence fields in the tropics (Julian 1980). The effect of the initialization on these fields depends very strongly on the type of interpolation that is used in taking the analysed data from pressure-coordinates to σ-coordinates.

The simplest method, direct interpolation of the analysed fields, enables the initialization to have a severely damping effect on the large scale tropical divergence field. Fig. 1a shows the initialized field of the zonally averaged meridional velocity, $[\bar{v}]$, in Starr's notation, for the operational analyses for November 1980. We note the very weak poleward flow near 150 - 200 mb and the alternation in the vertical of the sign of the velocity. Fig. 2a shows the monthly mean velocity potential at 150 mb for the same month (our sign convention is that the divergent wind blows across the isolines from low values to high. The contour is 10^6 m^2/sec so that 1 contour interval over 10^o latitude corresponds to 1 m/sec. We see that the initialized $\bar{\chi}$ is extremely weak. We made a change in the operational interpolation procedure in early December 1980 so that we interpolated from p to σ only the changes made by the analysis (interpolation of increments). This had a big effect on the

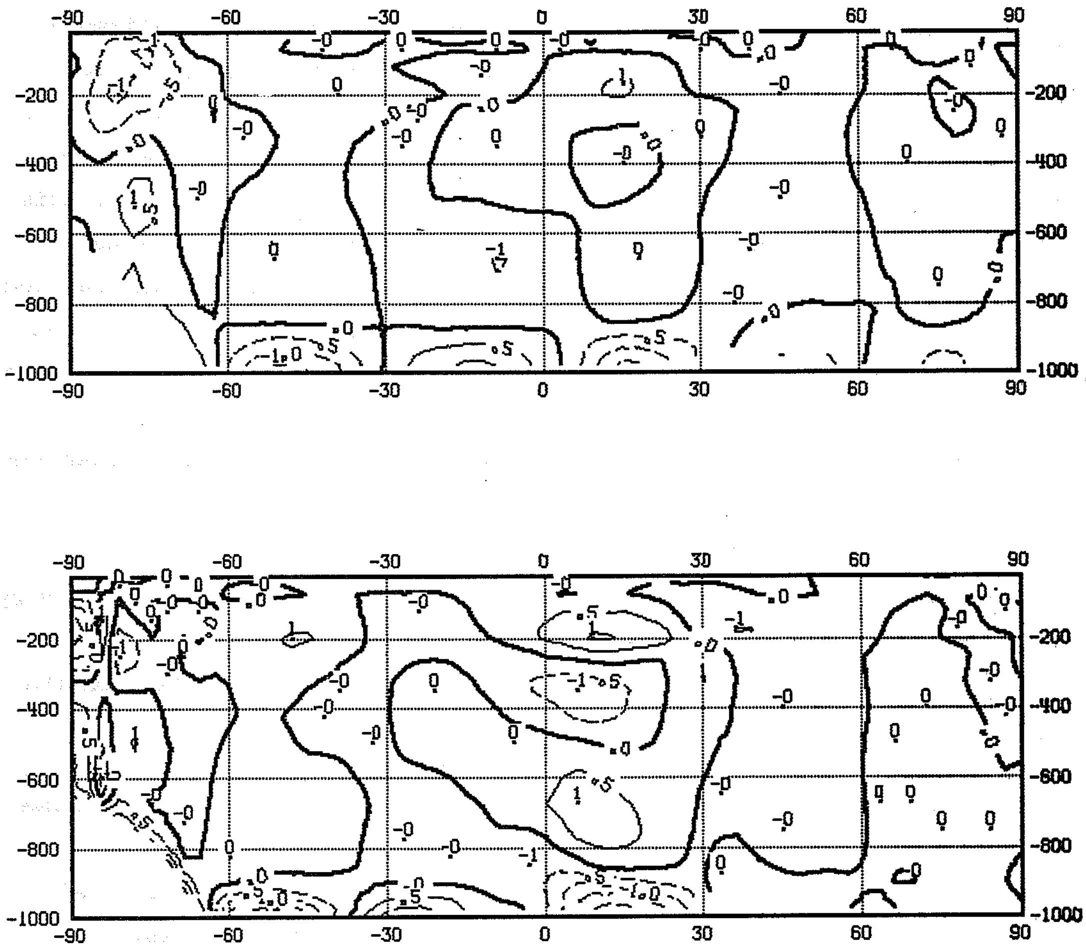

Fig. 1 Mean meridional velocity, $[\bar{v}]$, for initialised analyses, November 1980 (top), December 1980 (bottom).

mean χ for December 1980 (Fig. 2b). However the effect on the zonal mean circulation is much less marked (Fig. 1b). Moreover the alternation in sign of $[\bar{V}]$ is seen to be more marked than in November (Fig. 1a). Fig. 3a,b shows the mean initialized velocity potential at 300 mb for November 1980 and December 1980. We notice that in the tropics the main change between the two months in the intensification of the convergence region over Indonesia. This convergence is believed to be spurious and to be an artefact of the initialization procedure.

Given the errors in the initialized fields in the tropics, is there any reason to believe that they are of importance for the mid latitude forecasts? Despite controversy over some aspects of tropical and extratropical interaction there is no controversy over the importance of the tropics in maintaining the zonal mean flow of the extratropics. Fig. 4 (due to Savijärvi) shows a spherical harmonic decomposition of the day 3 forecasts for November 1979. We note the large concentration of error in the long waves (n = 4 to 8). The largest single contribution to the error is in the zonal flow, P_6^o.

Fig. 5 shows the structure of the mean zonal flow error for day 7-10 of the forecasts from December 1979. This is a characteristic error structure which we see every month in the forecasts, and which grows throughout the ten day forecast period. It also has the sort of structure in the north south associated with a P_6^o height field.

It is interesting to compare the structure of the forecast height error in Fig. 4 with Fig. 6 which shows the spherical harmonic distribution of kinetic energy in the divergent wind at 200 mb for January 1979, in the FGGE year. (Kanamitsu, pers.comm). There is a strong concentration of amplitude in the long waves and we note that P_6^o is again an important contributor.

It is tempting to speculate that there is some connection between the fact that the initialization damps the divergence in the initial data and the subsequent growth of important errors in the zonal mean flow.

2. EFFECT OF THE INITIALIZATION ON UNFORCED GRAVITY WAVES

The effect of the initialization is most simply discussed using the equation (Machenhauer 1977)

$$\dot{y} = i\sigma y + f \qquad (1)$$

to describe the evaluation equations of the model. Here y represents a single linear mode, $i\sigma y$ represents the linear terms of the equations and f represents the forcing of that mode from all other effects.

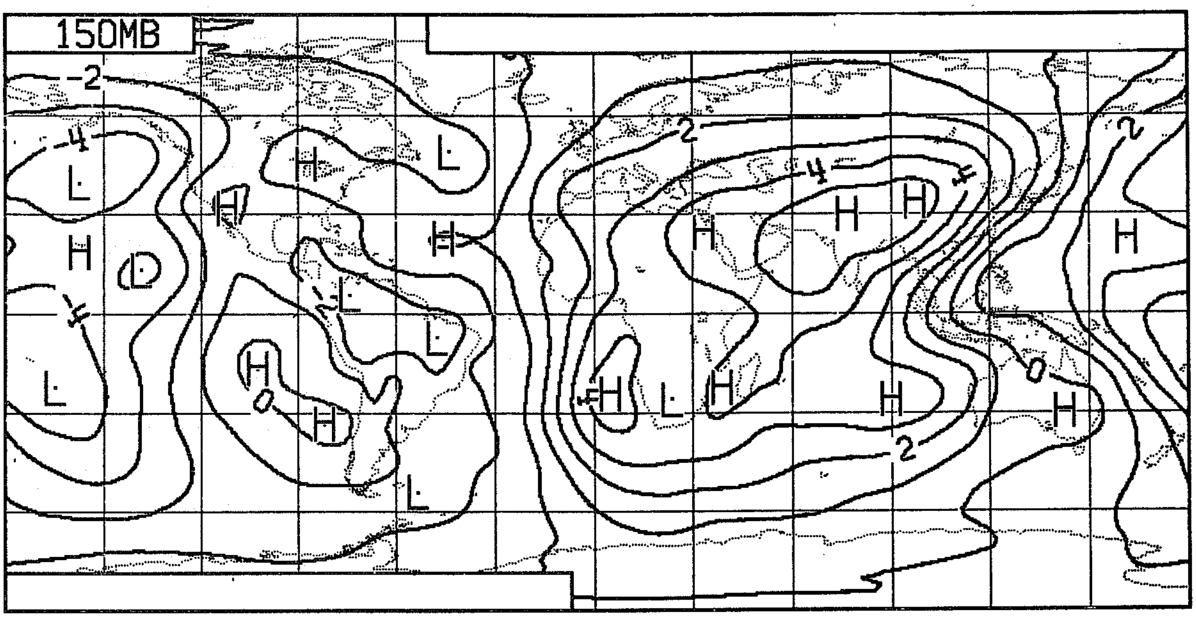

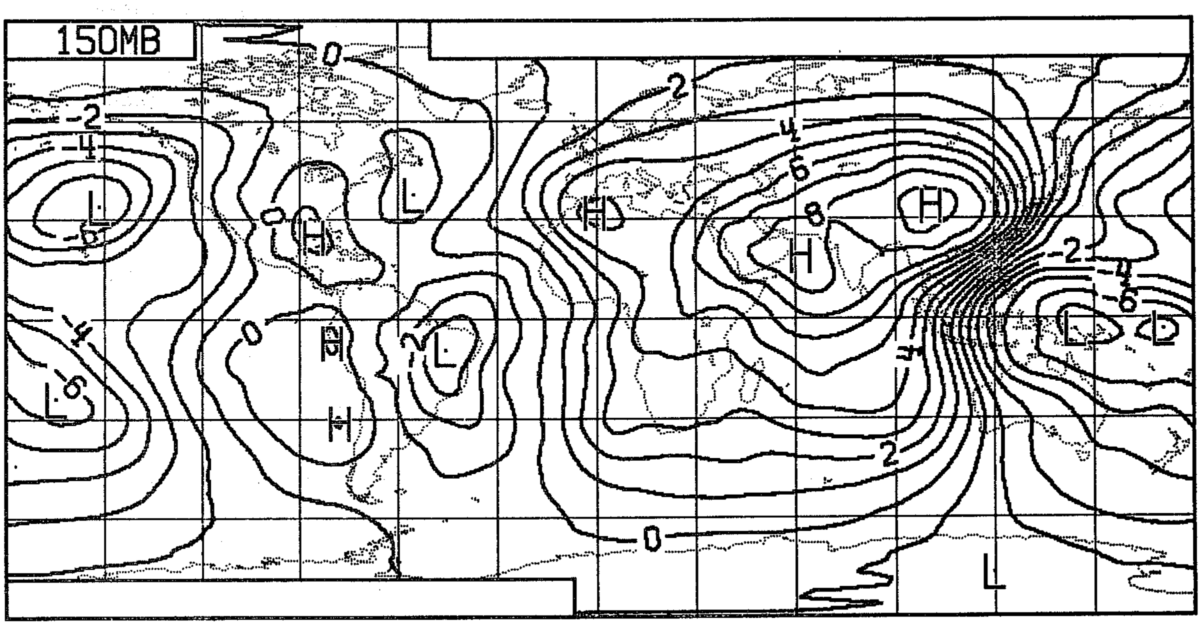

Fig. 2 Monthly mean velocity potential at 150 mb for initialised analyses, November 1980 (top), December 1980 (bottom). Contour interval $10^6 m^2 sec^{-1}$. The sign convention is such that the divergent wind blows from low to high values.

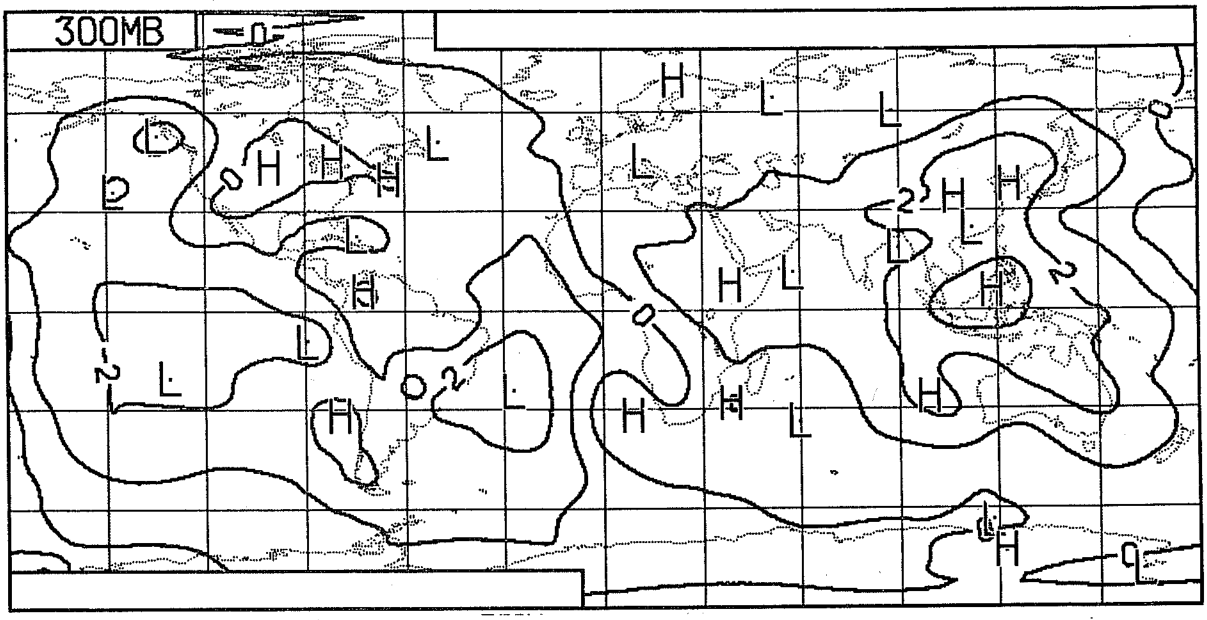

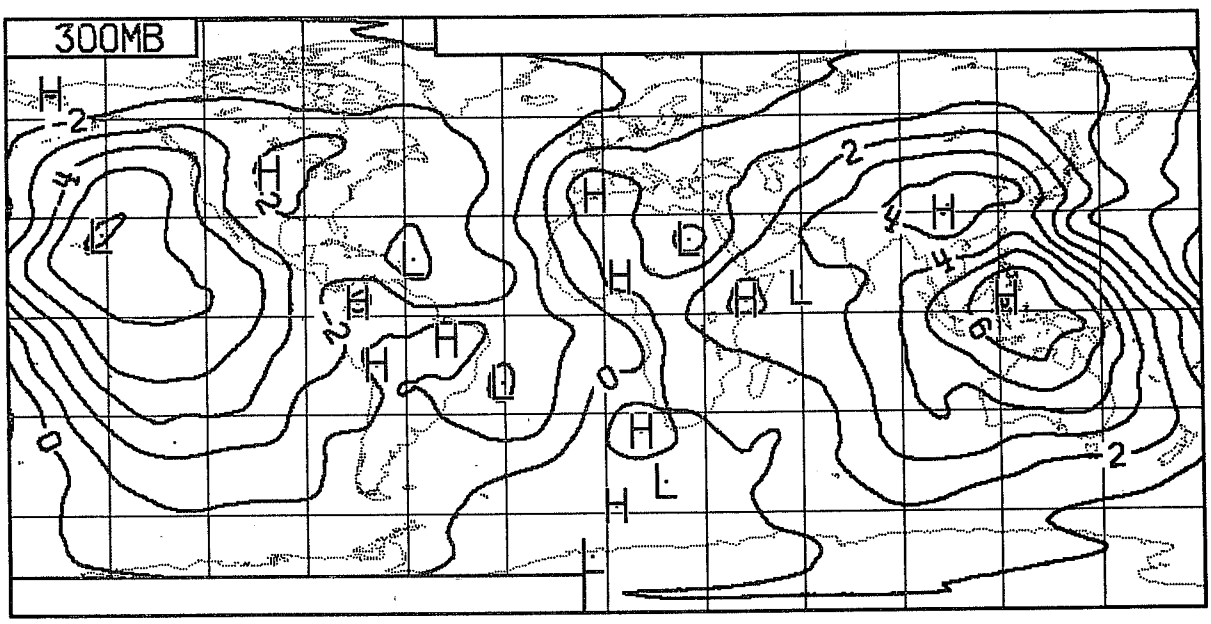

Fig. 3 As for Fig. 2 but for 300 mb.

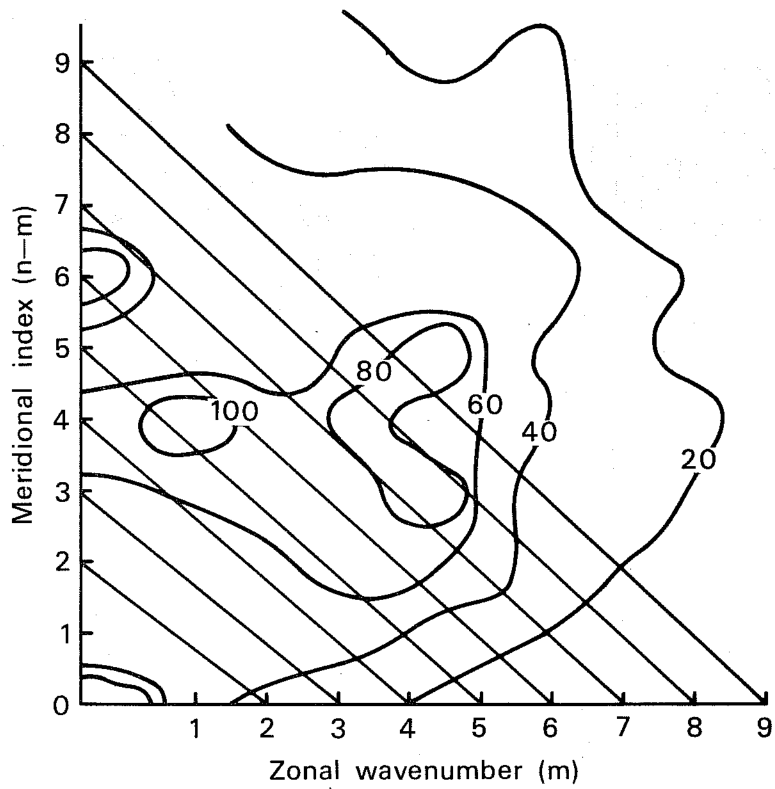

Fig. 4 Global spherical harmonic decomposition of the variance of the geopotential height errors for day 3 forecasts for November 1979. The abscissa is the zonal wave number, the ordinate the meridional index and the diagonal lines indicate the total wave number. The unit is m^2.

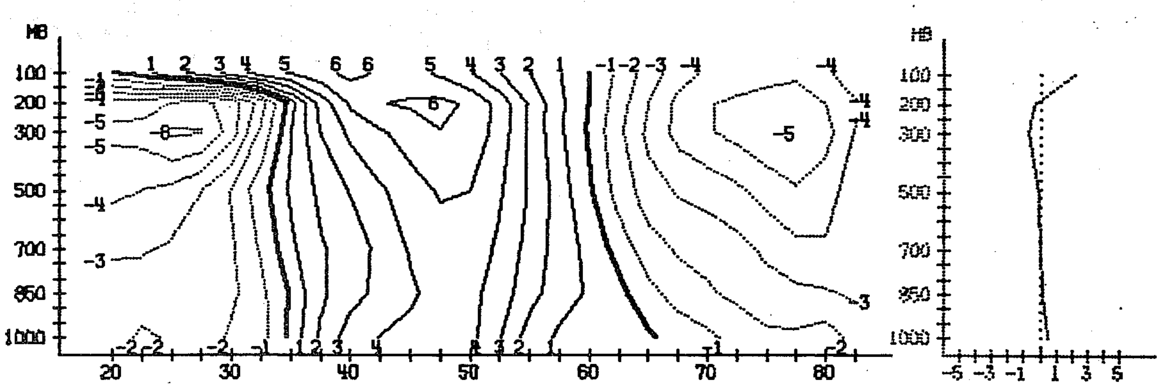

Fig. 5 Latitude height cross-section of the monthly mean error (forecast-observed) in the zonal wind, averaged days 7 to 10 of the operational forecasts for December 1979. Contour interval is 1 m/s.

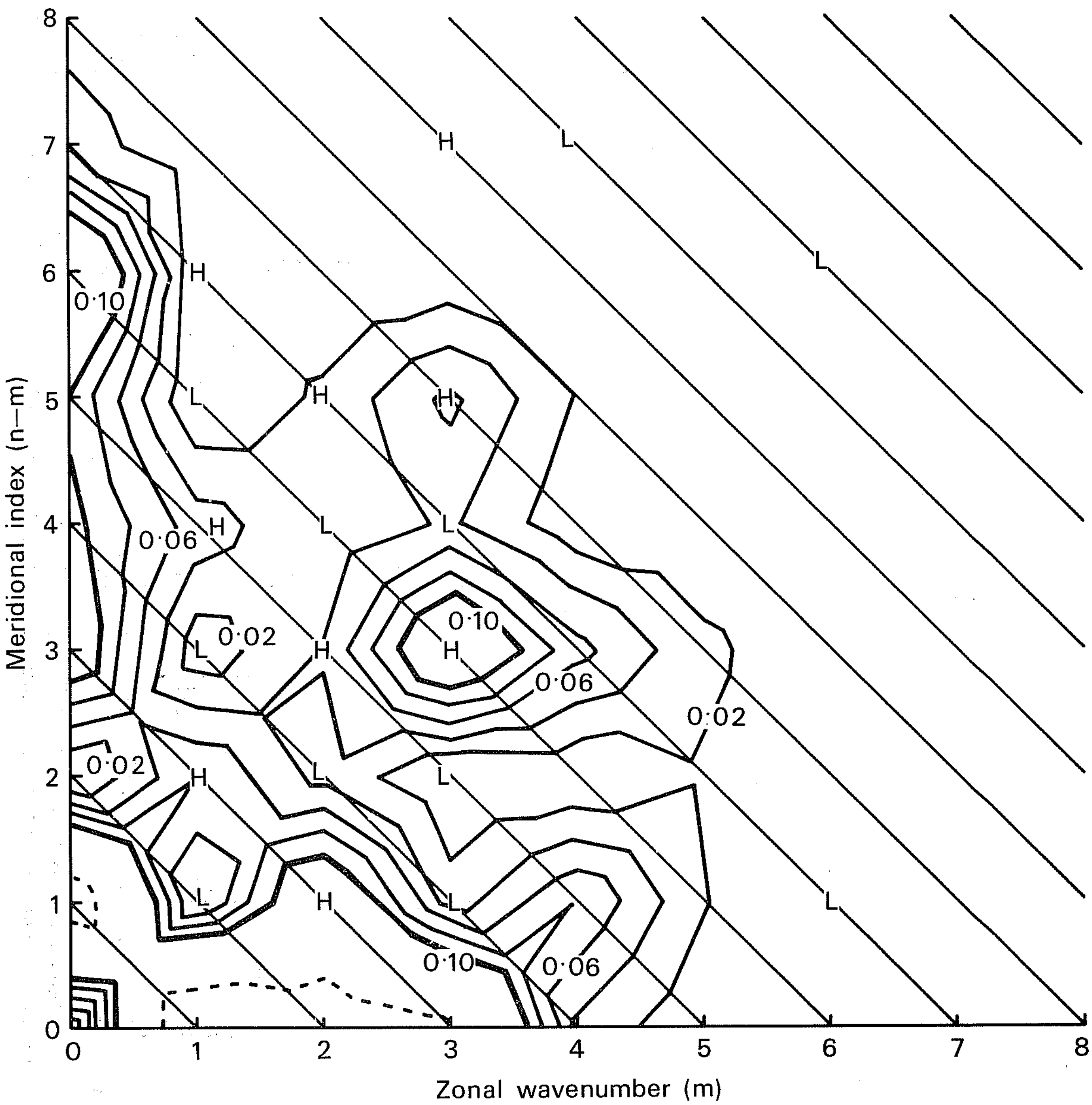

Fig. 6 Spherical harmonic spectrum of the kinetic energy of the 200 mb divergent wind for January 1979.

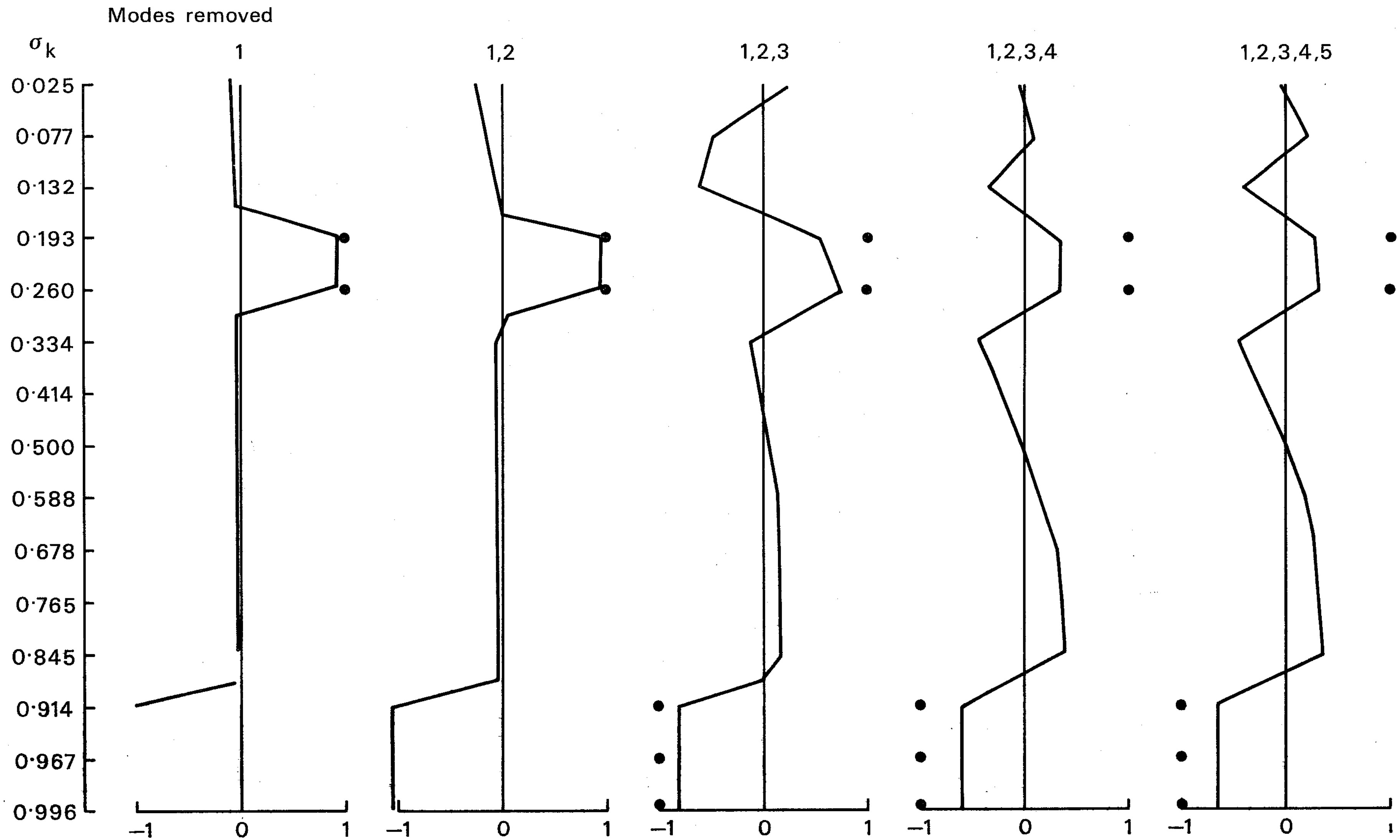

Fig. 7 Residual of a flow with low level inflow and upper troposphere outflow if we successively put to zero the contributions of mode 1 (left), modes 1 and 2 ... modes 1 through 5 (right). The dots indicate the original amplitude.

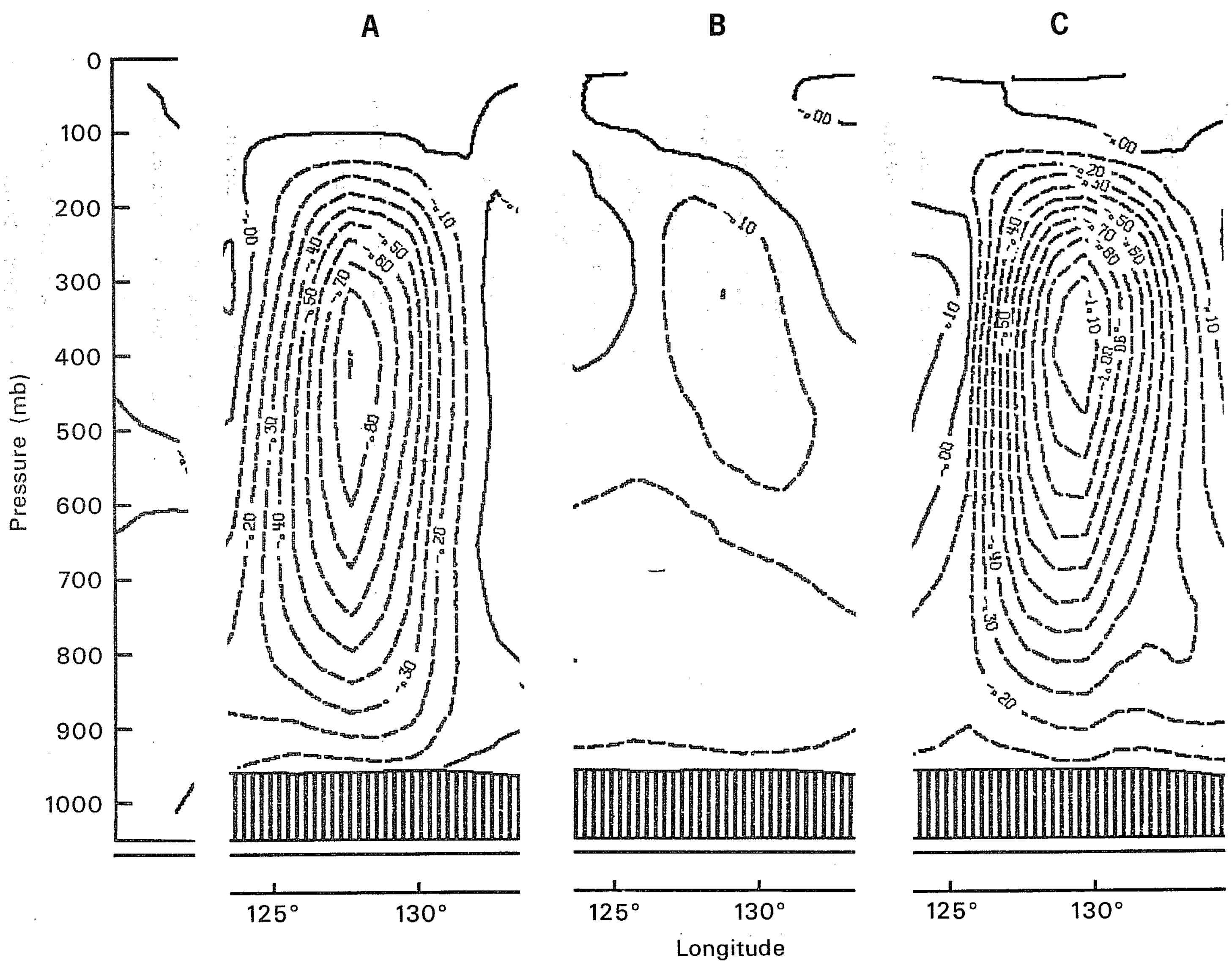

Fig. 8 Operational cross-sections of the ω-field along 27°S between 125°E and 135°E on 11 Dec. 1980
a) Uninitialised analysis 0600 GMT b) Initialised analysis 0600 GMT
c) 6-hour forecast at 1200 GMT. The contour interval is 0.1 Pa/s.

Assuming that f is constant (effectively, that it is slowly varying) the solution is

$$y = (y_o + \frac{f}{i\sigma})e^{i\sigma t} \quad \frac{f}{i\sigma} \tag{2}$$

The idea of the normal mode initialization is to adjust the initial amplitude y_o of each gravity mode so that

$$y_o + \frac{f}{i\sigma} = 0 \tag{3}$$

and then iterate the procedure. The intent is that the rapid variations associated with the $e^{i\sigma t}$ term are eliminated and one is left with the steady (i.e. slowly varying) forced term. Clearly, if the forcing f is zero then the effect of the procedure will be to put the initial amplitudes of the gravity wave components to zero.

In mid latitudes the forcing of the gravity modes from the Rossby modes is large, but this is not the case in the tropics. Thus to preserve divergence in the tropics one should either include the diabatic forcing in the initialization calculation or one should not initialize. The first alternative is apparently attractive. However there are reasons why it might be a little dangerous to do this in our present circumstances. These have to do with certain properties of our convection scheme and will be discussed below.

Here we consider the second possibility, i.e. reducing the effect of the initialization by doing it on fewer modes.

The Centre's model has fifteen levels in the vertical and so there are fifteen vertical modes. Currently in the initialization procedure we initialize all horizontal modes for the five gravest vertical modes (modes 1-5).

Modes 1-5 correspond to the external mode and the first four internal modes. Of these, mode 2 has one change of sign near 100 mb and cannot see any structure in the troposphere. Modes 3,4,5 have two three and four zero crossings respectively and so can indeed see structure in the troposphere.

The major effect of initializing modes 1 and 2 is to eliminate noise in the surface pressure tendency. Typically, uninitialized data can have initial surface pressure tendencies of as much as 25 mb/3 hr. The external mode is the major contributor but the contribution of the second mode is not insignificant. The higher modes typically contribute little to the surface pressure tendency. As more vertical modes are initialized the amplitudes in the vertical velocity are progressively damped. The fact that this has little effect on the surface pressure tendency indicates that the vertical integral of the divergence is not seen by these modes.

Let us now consider what happens during the initialization to a structure (e.g. the Hadley cell or a hurricane) which has low level inflow and high level outflow and which the adiabatic initialization perceives as an unforced gravity wave. Since there is no forcing the initialization will set to zero the amplitude of each of the vertical modes being initialized. In the Centre's σ-coordinates let us suppose unit inflow occurs at the lowest three levels (σ = .915, .965, .996) and that unit outflow occurs at levels three and four (σ = .193 and .260). Fig. 7 shows what happens when we progressively put to zero mode 1, modes 1 and 2, etc. up to modes 1 to 5 (the major contributors to the structure are modes 3, 4 and 7). We can see that "initialization" of modes 1 and 2 has little effect, initialization of mode 3 produces a large change in the stratosphere while "initialization" of mode 4 produces a significant change at σ = .334 while cancelling part of the change in the stratosphere caused by "initializing" mode 3.

The conclusion from Fig. 7 is that if one wants to preserve inflow-outflow structures of the kind discussed while reducing the noise in the surface pressure tendency then one should only initialize the first two modes. Unfortunately the convection scheme in the Centre's model has a tendency to generate grid point storms not only in the forecasts but also, occasionally, in the data assimilation. Without some form of control this could perhaps lead to incorrect rejection of good data. Fig. 8 shows the vertical cross-section of the ω field in one such storm over Australia in December 1980. At the time there was wide spread convection over the western part of Australia as the monsoon set in. Fig. 8a shows the uninitialized vertical velocity at 0600Z, with a maximum value of .9 Pa/sec at 400 mb. Fig. 8b shows the initialized vertical velocity where the ω structure has been destroyed and Fig. 8c shows the succeeding 6 hour forecast where the storm has re-developed with ω in excess of 1.1 Pa/sec.

3. EXPERIMENT WITH REDUCED NUMBERS OF MODES INITIALIZED

For the reasons cited above we decided to compromise, and taking account of the spectrum of divergent kinetic energy we made an assimilation and forecast experiment where we initialized five vertical modes for all wavenumbers higher than zonal wavenumber 7 and only two vertical modes for all lower zonal wavenumbers including of course m = 0.

3.1 Data assimilation

The experiment was run for 5 analyses (4x6 hour cycles) from 12Z on 21/1/81 to 12Z on 22/1/81. The control run used the operational system of initializing 5 vertical modes at all zonal wavenumbers. The most serious matter for the data assimilation, when any changes are made, are differences in the rejection rates of data and differences in the analyses. The data rejected in both the control and the experimental assimilations were almost identical. In any automated checking system there are always some data which are borderline for acceptance or rejection. Any change in the system will always lead to some change in the data rejections. In this case there were only a few changes in rejection, mostly in the extratropics. In the last analysis, 12Z on 22/1/81 four or five more surface observations were accepted that were rejected in the control run while four or five data at 850 mb that has previously been accepted were now rejected.

The effect on the divergence field was in that sense expected. Fig. 9 shows the zonally averaged meridional velocity [V] in the two initialized analyses. The northern hemisphere trade wind inflow to the equator has deepened and intensified while the upper level outflow is dramatically different. It should be pointed out that three geosynchronous satellites were operational, while the radiosonde and polar orbiter coverage was normal, so that the analysis of the divergent wind is probably fairly reliable.

Fig. 10 shows the initialized velocity potential at 150 mb in the two runs. There is not a lot of difference in the Australia/Indonesia/Siberia region. However there are significant differences in the region between West Africa and Hawaii. Here the tropical circulation in the experiment is much more intense than in the control and there is no difficulty tracing the ITCZ outflow around most of the globe. The strong divergences over South America is particularly noticeable.

At 300 mb (Fig. 11) the large convergence area over Indonesia/Australia in the control run has been replaced by an area of divergence which again is desirable.

At 850 mb, Fig. 12, there are again significant differences in the large scale velocity potential field. The convergence over Indonesia and South America has been considerably enhanced as has the divergence from the sub-tropical high along the west-coast of Africa and North America.

Fig. 13 shows the difference between the 1000 mb geopotential (i.e. $z_{control} - z_{expt}$) in both the northern and southern hemispheres in the section between 90E and 90W for the northern and southern hemispheres separately. The main differences, as usual, are in the data sparse areas and do not exceed 12 m (i.e. 1.5 mb). In the extratropics the differences can be explained in terms of differences in data rejection and are typically of small scale.

The largest scale differences, also of order 10 m, occur along the equator. Since pressure at the equator is higher in the east Pacific than in the central Pacific the experiment shows a larger pressure gradient, favouring easterlies along the equator, then the control run between 80W and 180W. This might be expected to have some effect on the forecast.

3.2 The forecast

Verification of the forecasts made with the ECMWF forecasting model from the two analyses showed very little difference in the northern hemisphere north of 20 N. The maps were similar and the verification statistics were similar. Fig. 14 shows the zonally averaged and time averaged (day 5 to day 10) difference between the mean zonal wind and analysis for the forecast run from the control analysis (E49) and the forecast run from the experimental analysis. Both plots together with Fig. 5 show why we speak of certain errors as systematic errors. Both forecasts are typical in the structure of the error of the mean zonal flow. Sadly there is very little difference between the errors in this field for the two models.

Perhaps the systematic errors are so dominating that we can only see sensitivity to the differences in the initial data in the early stages of the forecast.

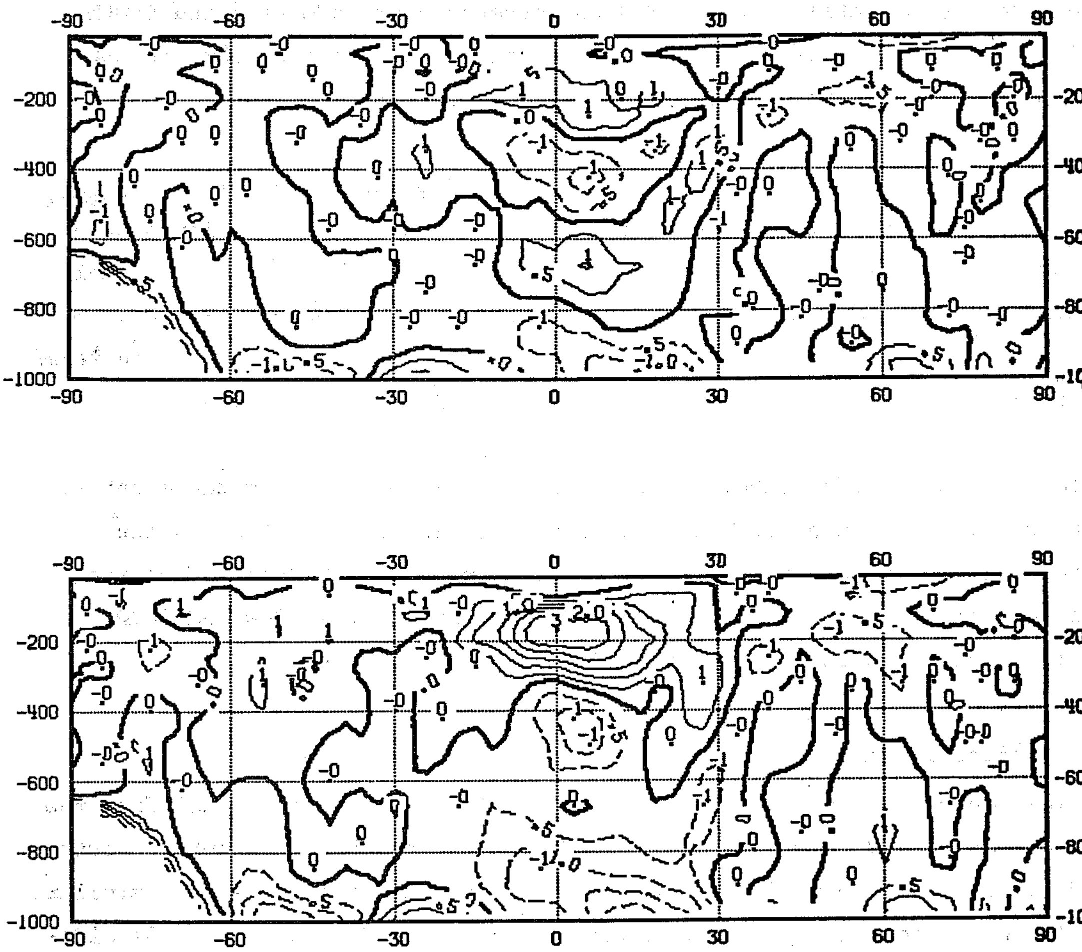

Fig. 9 Zonally averaged $[\bar{v}]$ in the initialised analysis in the control run (top) and in the experiment (bottom) after one day of assimilation. Contour interval is 1 m/s.

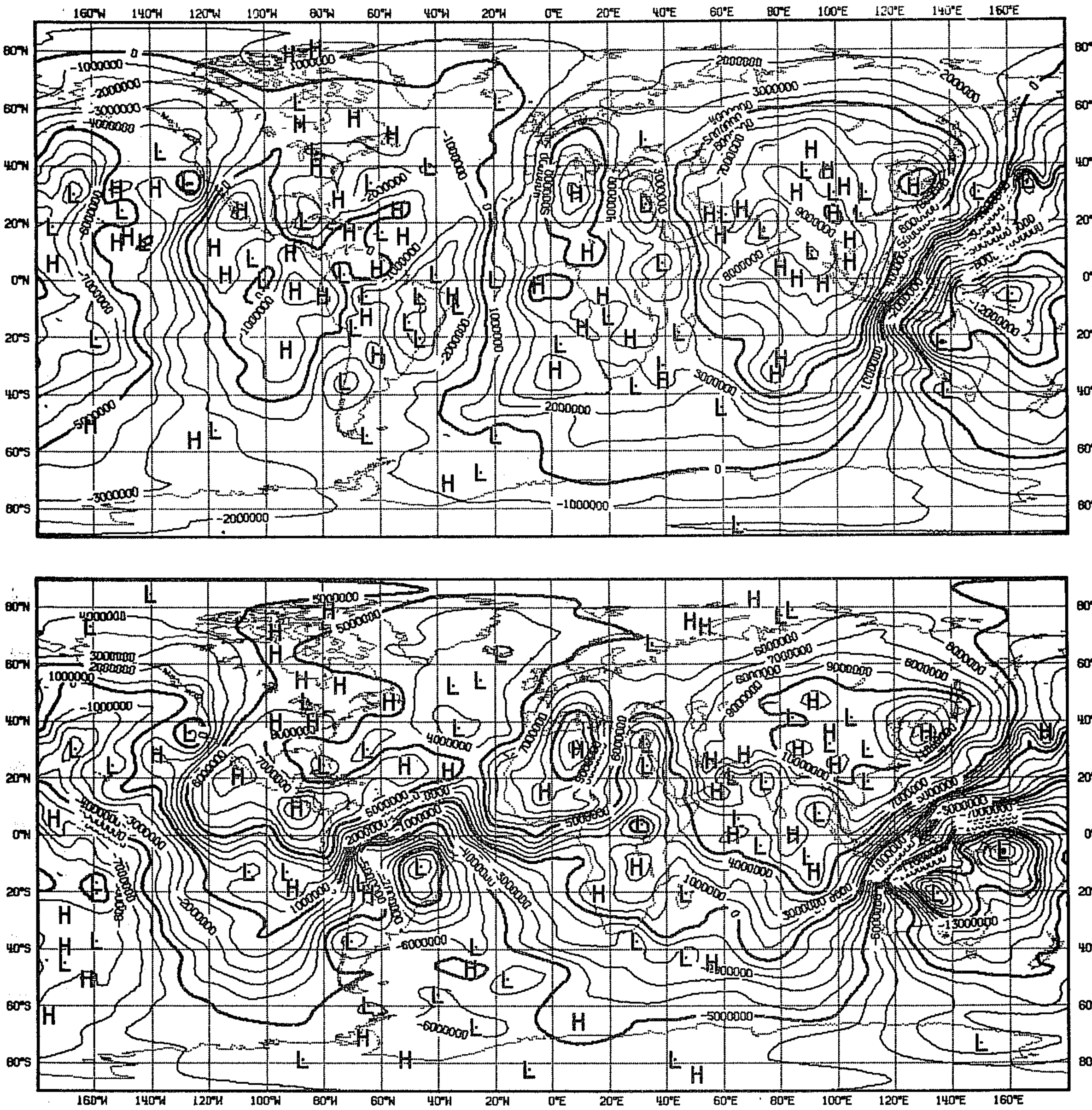

Fig. 10 Velocity potential at 150 mb in the control run (top) and the experiment (bottom) after one day of assimilation.

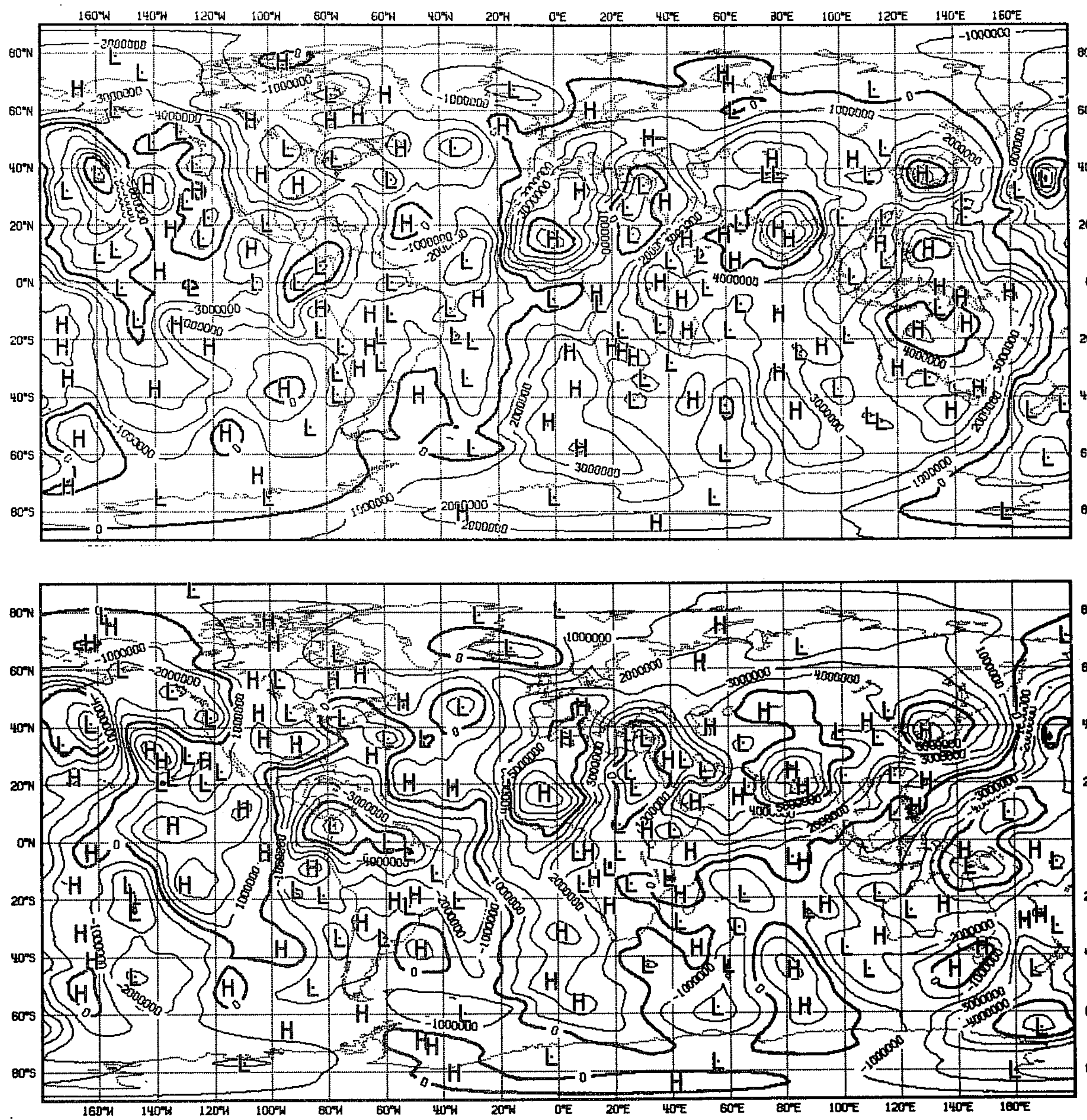

Fig. 11 As Fig. 10 but for 300 mb.

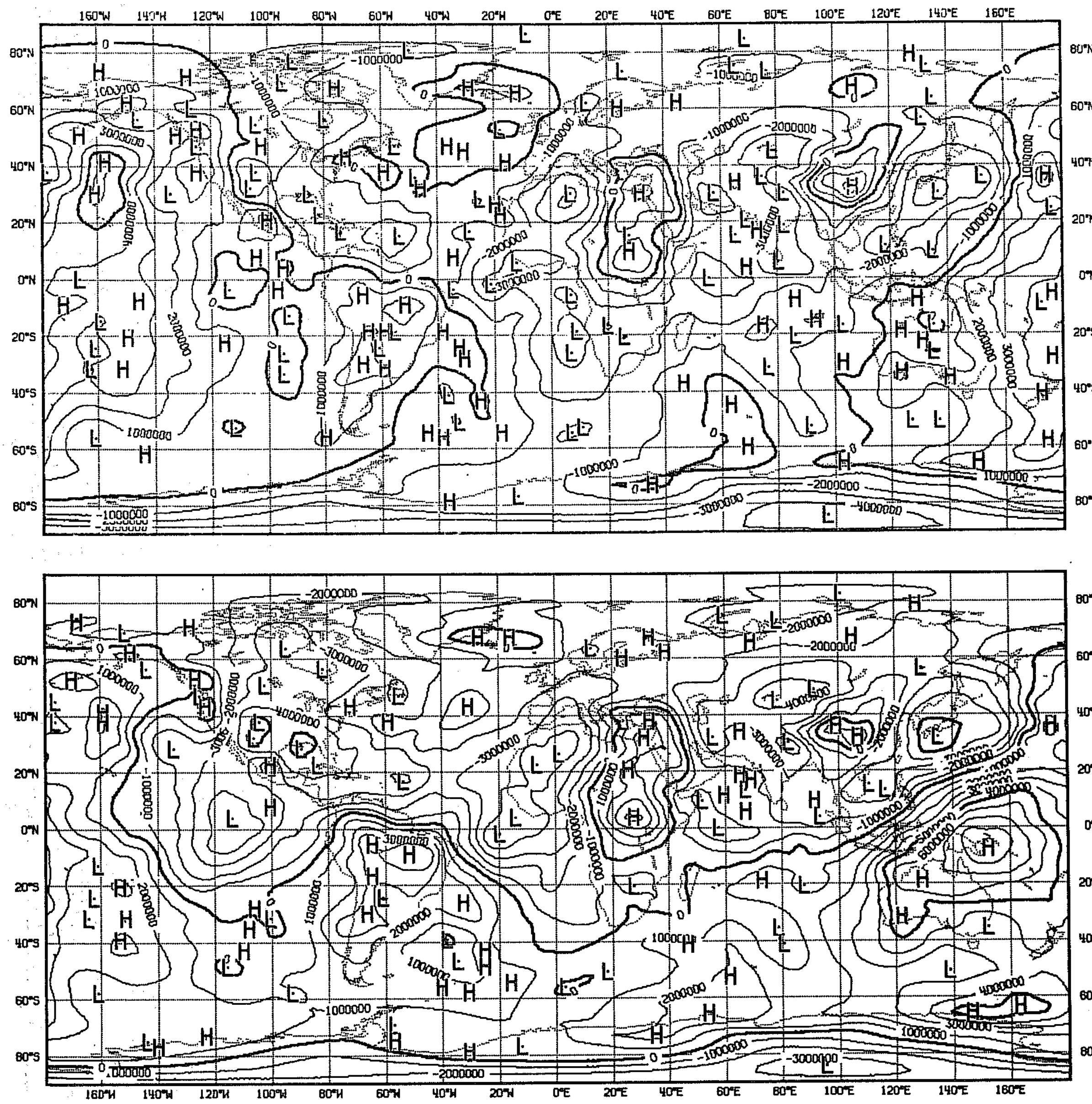

Fig. 12 As Fig. 10 but for 850 mb.

Northern Hemisphere

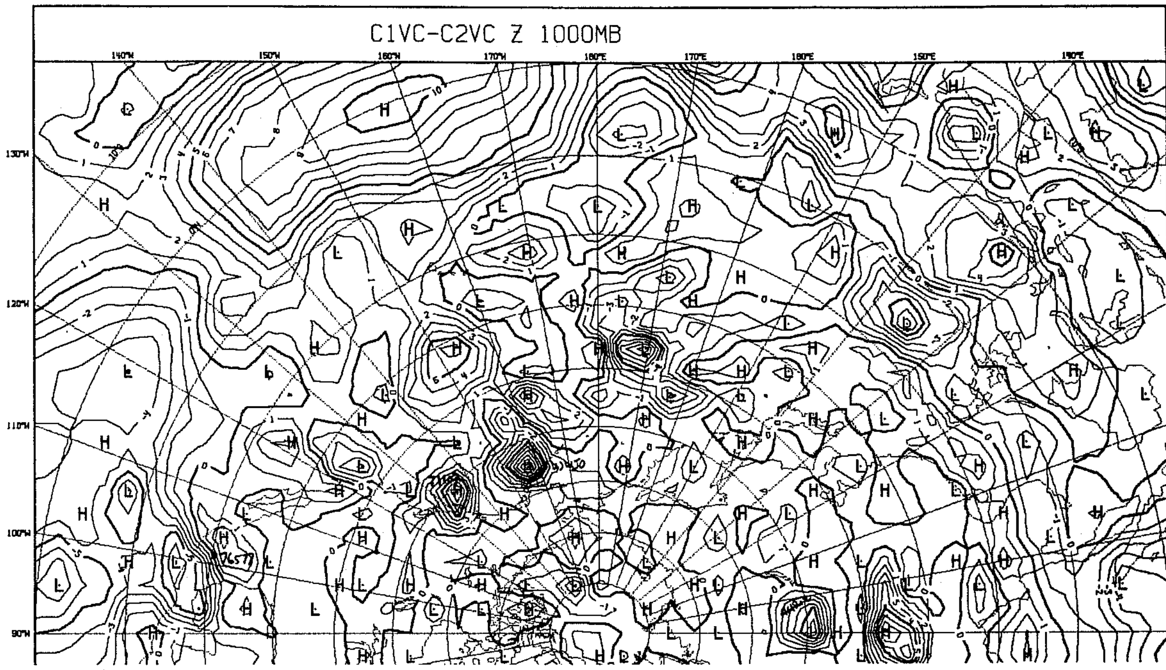

Southern Hemisphere

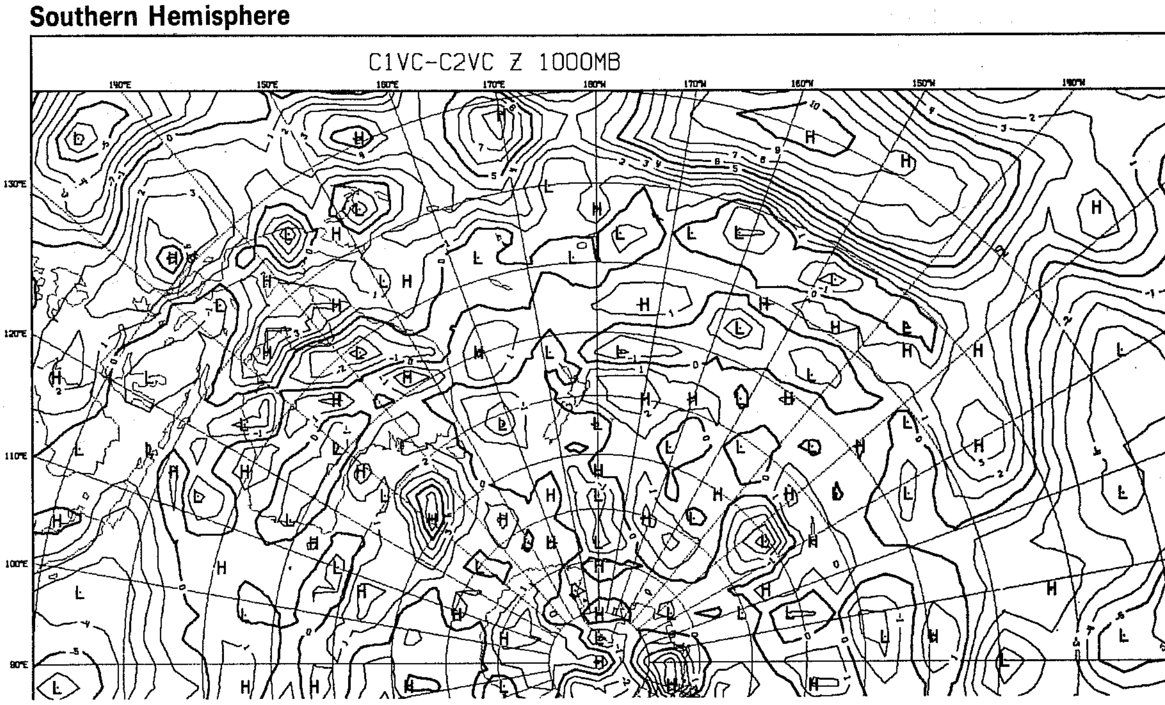

Fig. 13 Difference between the height fields at 1000 mb (z control - z experiment) in the northern (top) and southern (bottom) hemispheres after one day of assimilation. The contour interval is 1 m.

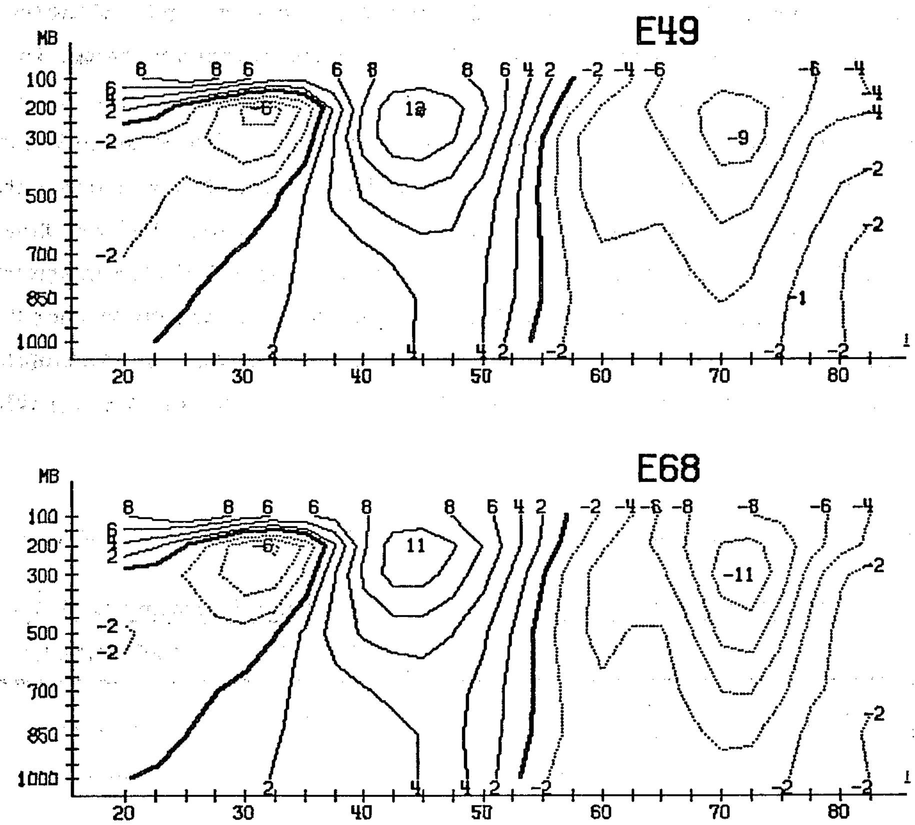

Fig. 14 Error in the zonal mean flow, averaged over the last five days of the forecast for control run (E43) (top), experimental run (E68) (bottom). Contour interval is 1 m s^{-1}.

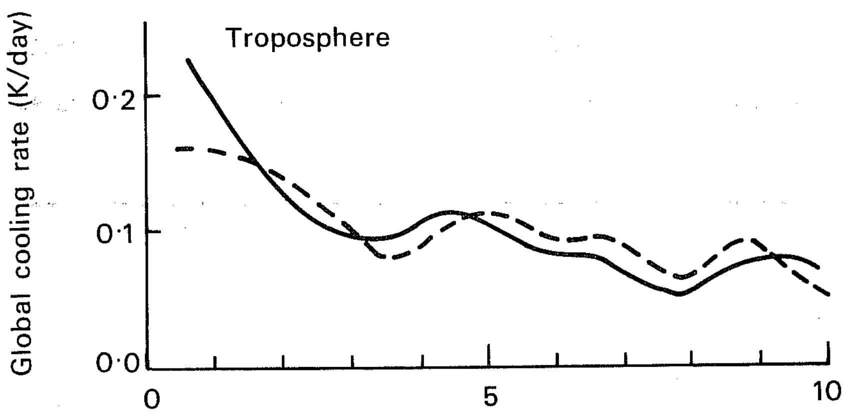

Fig. 15 Global tropospheric cooling rate (deg/day) for the control (——) and experimental (----) forecasts.

Table 1 shows the evolution with time of the total convective and radiative heating in the model for the two runs. These are the two largest terms in the global heat budget. The evolution of the radiative cooling rate is very similar in the two runs. However there is a significant difference in the convective heating rate in the first day. The spin up time for the convection is appreciably shortened by about twelve hours. The effect of this is shown by the tropospheric (i.e. below 160 mb) cooling rate, Fig. 15. The systematic cooling during the forecasts results from an inadequate release of latent heat. We see that the change in the initial data has an effect on the tropospheric cooling rate in the first day only. Thereafter the two runs are very similar.

Table 1. Global heating rates dur to cumulus correction and radiation

	cumulus heating (W/m^2)		radiation cooling (W/m^2)	
Hour	Control	Experiment	Control	Experiment
0-6	35.6	43.3	101.0	100.6
6-12	42.3	48.3	100.3	99.8
12-18	43.9	48.5	99.5	99.1
18-24	46.4	51.9	99.3	99.0
24-36	49.7	49.9	98.8	98.7
36-48	52.3	51.2	98.0	97.7
48-60	55.0	53.6	97.0	91.7
60-72	55.0	53.6	96.1	95.8
72-96	51.0	52.2	94.7	94.3
96-120	48.2	47.2	93.1	92.6

Does this mean that the model can recover quickly from the presumed ill-effects of the lack of divergence in the initial data of the control run? That is suggested by the cooling rate and also by Fig. 16 which shows the plot of $[V]$ at day 1 for the two experiments. The fields of $[\bar{V}]$ at day 1 are much more similar than they were at the initial time; the Hadley cell appears to have spun up satisfactorily. We turn now to look at the tropical forecasts to see if this is borne out by the flow fields.

Fig. 17 shows the day 3 850 mb streamfunction field in the two forecasts and in the verification (the contour interval is 10^7 m^2 s^{-1} so that one interval in 10° latitude corresponds to 10 m s^{-1}). Between 30N and 30S the forecasts look very similar and share a number of serious errors. The cyclonic disturbance in South Africa was missed in both forecasts. More seriously however we note the change in direction of the trade winds in the East Pacific in both forecasts together with the southward shift of the tradewinds in the Atlantic. That this is not a-typical is suggested by Fig. 18 which shows the mean streamfunction for the December analyses and for the three day forecasts in December. In these means we see that the subtropical anticyclones of the southern hemisphere (marked by L "low" in the streamfunction field since they are in the southern hemisphere) are seriously weakened by day 3 with a consequent serious weakening, by at least a factor of 2, of the trade winds in all three oceans. If we examine the 850 mb velocity potential fields at day 3 (Fig. 19) in our two forecasts, there is no sign whatever of the substantial differences we saw in the initial data. By and large the fields are very similar with the control forecast (E49) being, if anything, a little more intense over South America.

Turning now to the 150 mb streamfunction field (Fig. 20) we see that again the forecasts are very similar. They have both done quite well on the trough at 20S, 120W although they both fail on the trough immediately to the south at 45S. Both forecasts weaken the low over north east Brazil and do not have enough amplitude in the cyclonic disturbance over South Africa. The northern hemisphere subtropical high north of Indonesia has weakened and moved eastward.

The mean errors in the 150 mb streamfunction forecasts at day 3 are harder to see at 150 than at 850 mb and so Fig. 21 shows the mean December analysis and mean day 5 forecast. The anticyclone over Latin America is moved south westwards and elongated; the trough in the tropical south Atlantic is weakened and disconnected from the extratropical flow, as happened in our two forecasts; and, unlike the forecasts, the anticyclone in the western Pacific weakens slightly but moves eastward.

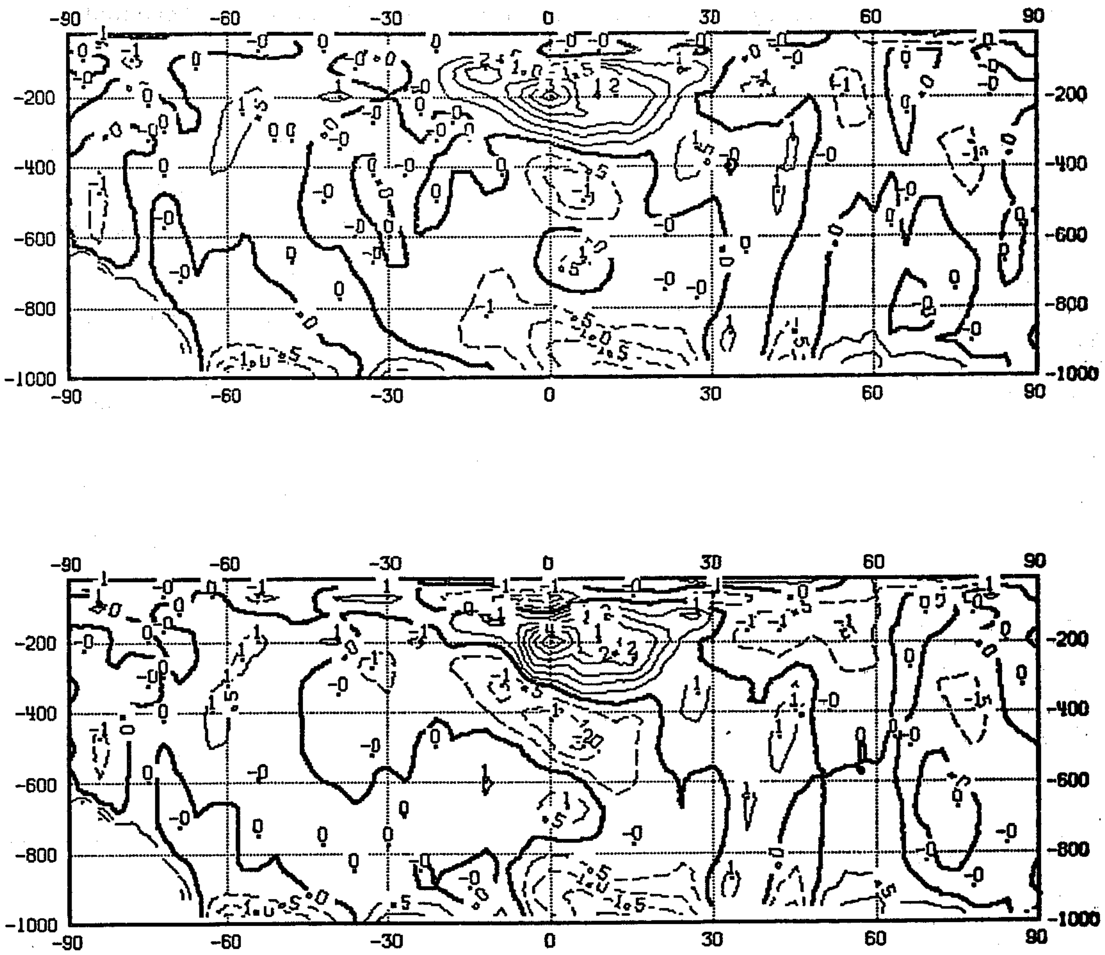

Fig. 16 Plots of the zonally averaged meridional velocity $[\bar{v}]$ at day 1 of the control (top) and experimental forecasts (bottom). Contour interval is 1 m/s.

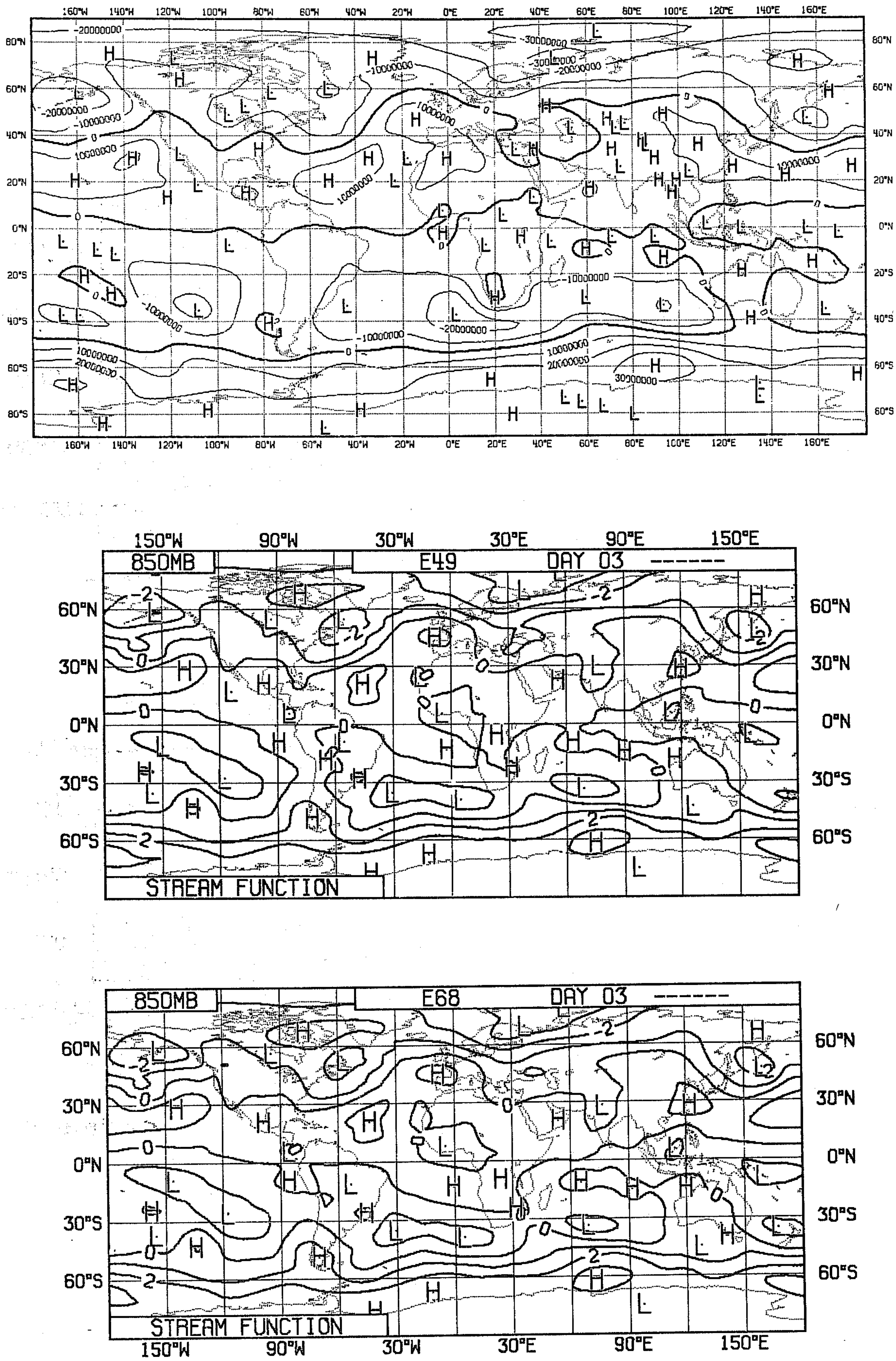

Fig. 17 Stream function at 850 mb for the verification (top), control (middle) and experimental (bottom) forecasts at day 3. Contour interval is $10^7\ m^2\ s^{-1}$.

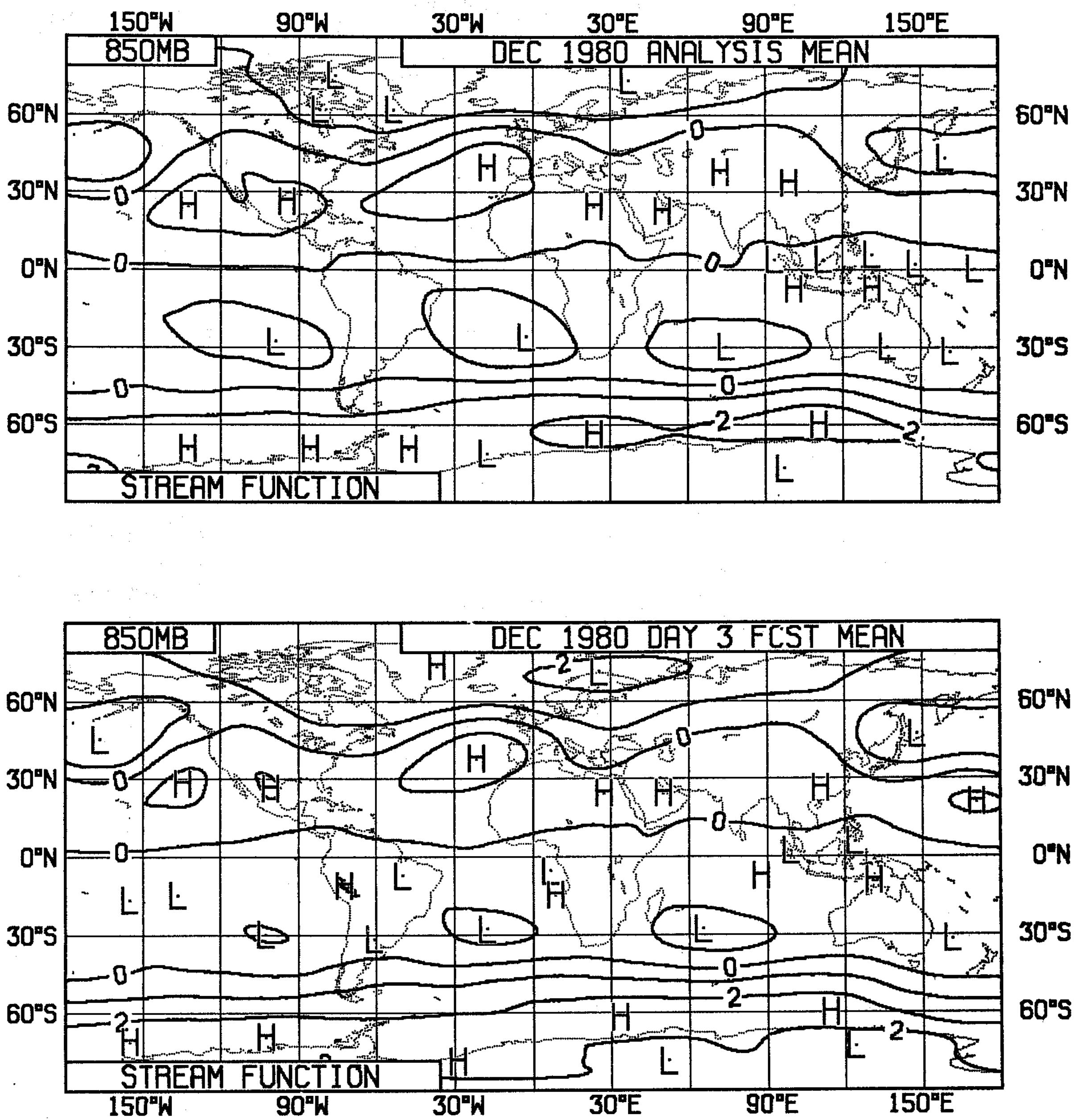

Fig. 18 Monthly mean of 850 mb stream function for December 1980 for analysis (top) and 3-day forecasts (bottom). Contour interval 10^7 m^2 s^{-1}.

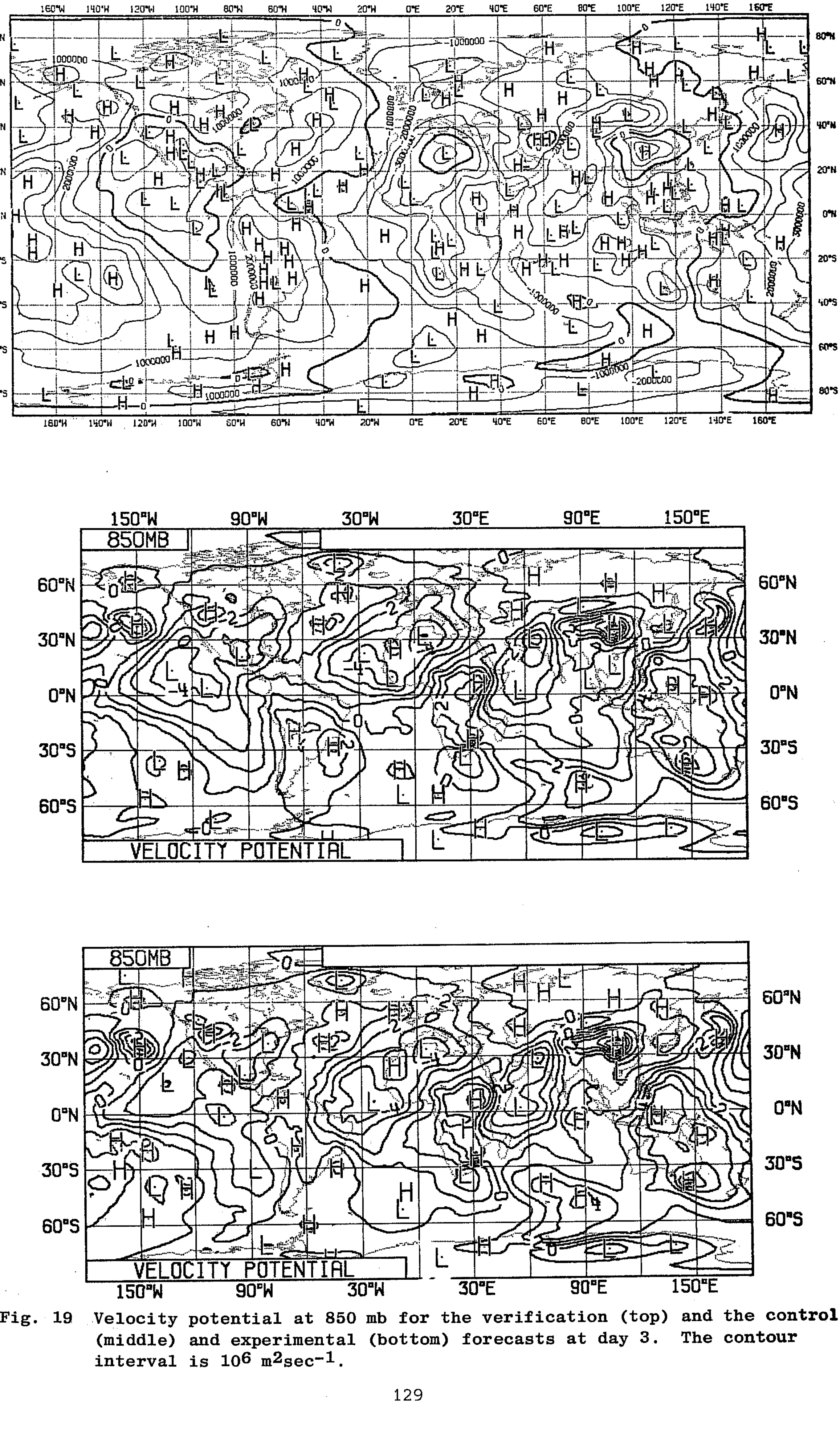

Fig. 19 Velocity potential at 850 mb for the verification (top) and the control (middle) and experimental (bottom) forecasts at day 3. The contour interval is 10^6 $m^2 sec^{-1}$.

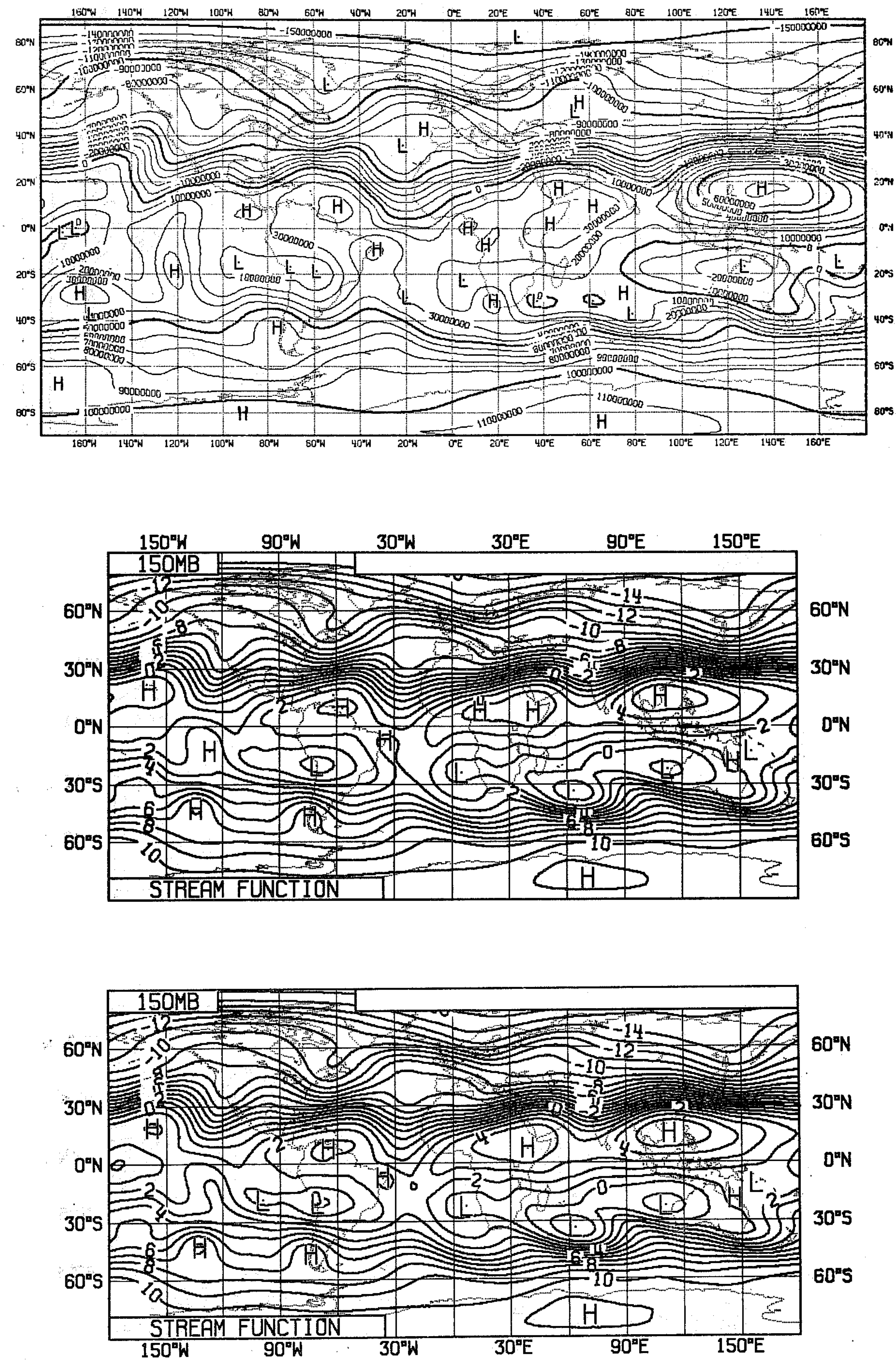

Fig. 20 As Fig. 10 for the stream function at day 3 at 150 mb. The contour interval is 10^7 m^2/sec.

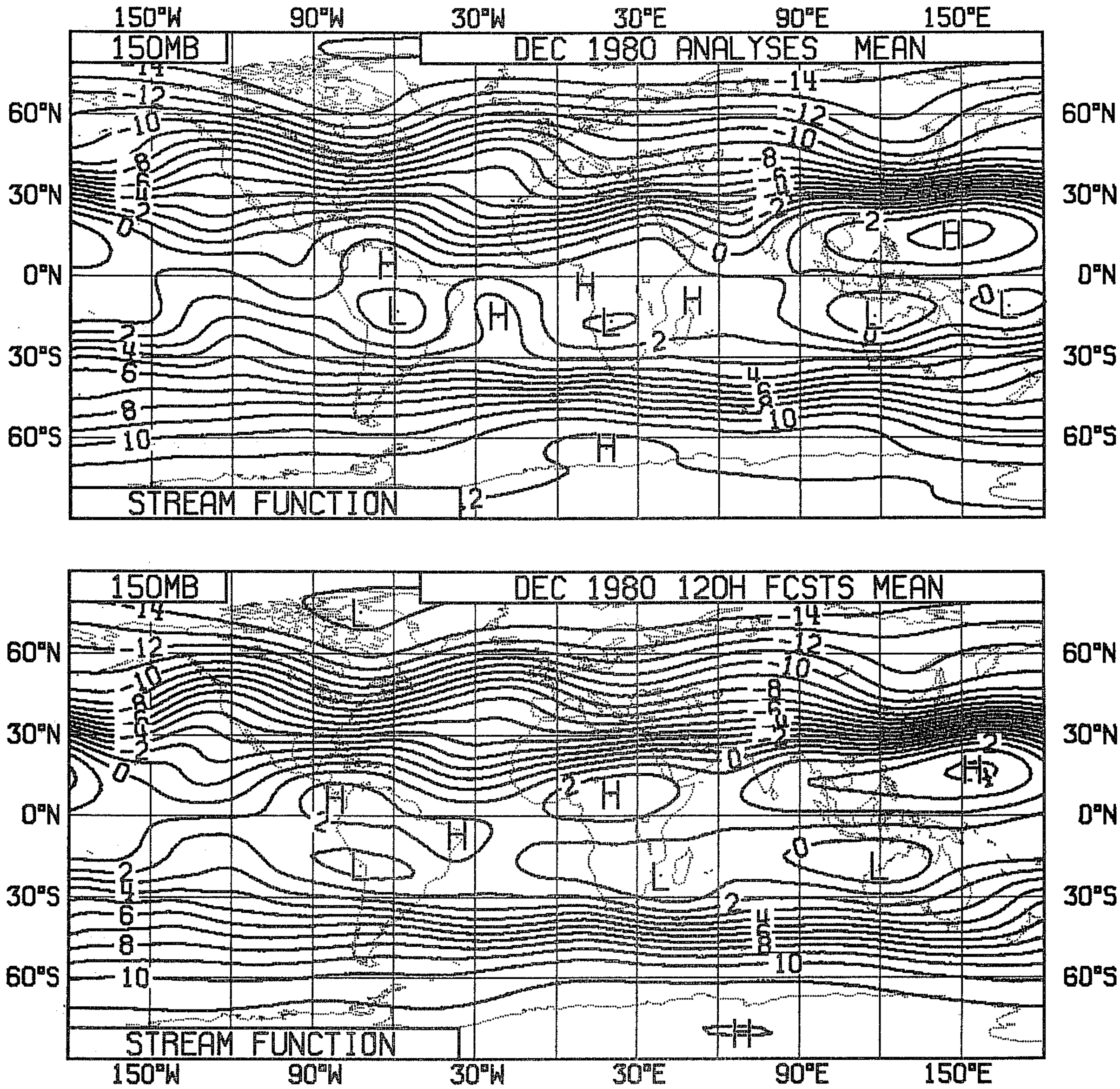

Fig. 21 Monthly mean of 150 mb stream function for the December analyses (top) and the day 5 forecasts (bottom). Contour interval is 10^7 m^2 sec^{-1}.

Thus we see that not only do these two forecasts but also most of our forecasts exhibit problems in maintaining the tropical circulation, in the first few days of the integration. It should be said that the trade winds do indeed recover their strength around day six in the mean of the forecasts. However the main feature of the tropical circulations, their steadiness, is certainly not forecast in the first few days.

4. POSSIBLE CAUSES FOR WEAKENING OF THE TRADE WINDS

It is by no means clear what is the reason for this serious failure of the trade wind forecasts in the first few days. An obvious candidate is the convection scheme. Fig. 22 shows the velocity potential in the December 1980 mean analyses and day 5 forecasts at 150 mb. We note the strong intensification of the Indonesian divergence centre and the suppression of the latin American divergence. In fact by day 10 the mean velocity potential field shows a pattern in which $P_1^{'}$ dominates with outflow occurring only over Indonesia (Kanamitsu, personal communication).

In order to investigate the behaviour of the convection in the present experiments we plotted for both experiments (Fig. 23) the initial meridional profile of the CAPE, cloud available potential energy (Moncrieff 1981) (CAPE = $\int_{bottom}^{top} \frac{g\Delta\theta}{\theta}\, dz$ where top, bottom refer to cloud top and bottom) averaged over conditionally unstable points. A typical observed value is a few hundred kg^{-1} while values in excess of 1000 Jkg^{-1} occur only in extreme situations (Miller and Moncrieff, personal communication). We see that the average values for both data sets in the tropics are very extreme, while individual values ranged up to 6000 Jkg^{-1}. The surprising thing however is that the value of CAPE had increased in the experiment, rather than decreased as one might have expected. The Kuo convection scheme requires net moisture convergence up to cloud top together with a conditionally unstable atmosphere in order to allow convective latent heat release. In the experiment run we had intensified the divergence field, enhanced the convection but also increased the CAPE.

In order to get an independent test of this result we took an operational forecast at random (February 10 1981 in fact) and plotted the CAPE values at day 0, day 2½ and day 6½ in the forecast (Fig. 24). Just as happened in the experimental assimilation the mean CAPE for unstable points increases from the beginning of the forecast at most latitudes. This is borne out by Fig. 25 which shows the number of points at each latitude which were conditionally unstable at days 0, 2½, 6½ in this same forecast. There are no significant changes through the forecast.

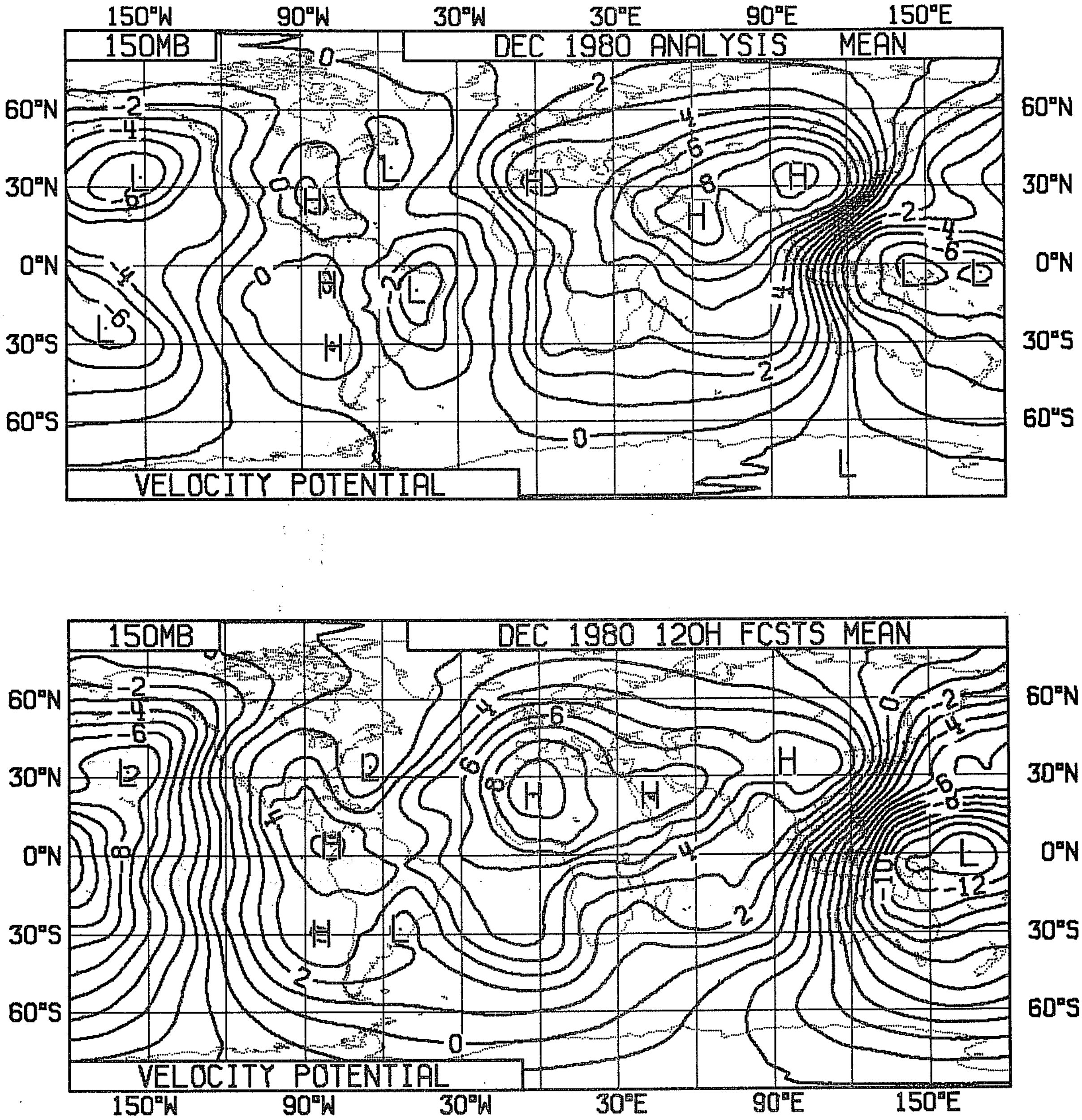

Fig. 22 As Fig. 21 for the velocity potential at 150 mb.

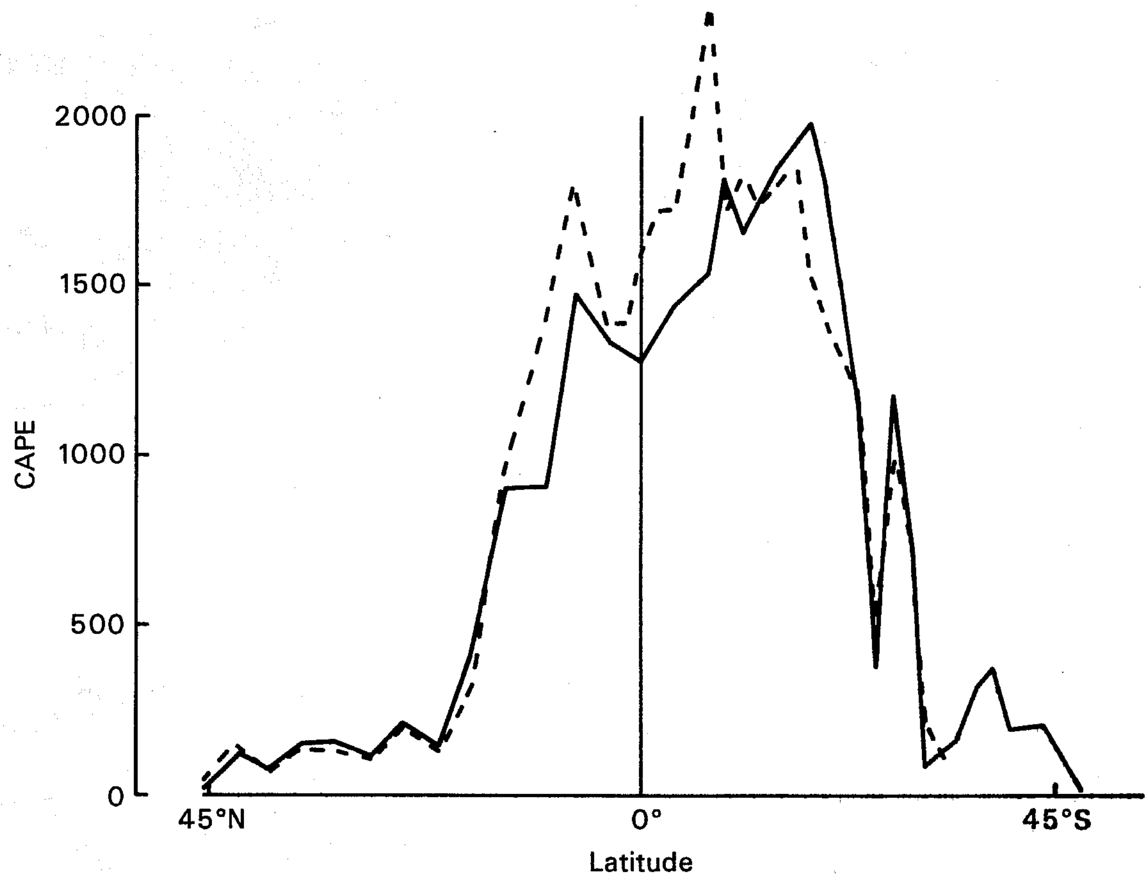

Fig. 23 Meridional profile of cloud available potential energy for the control analysis (——) and experimental analysis (----). The units are J kg^{-1}.

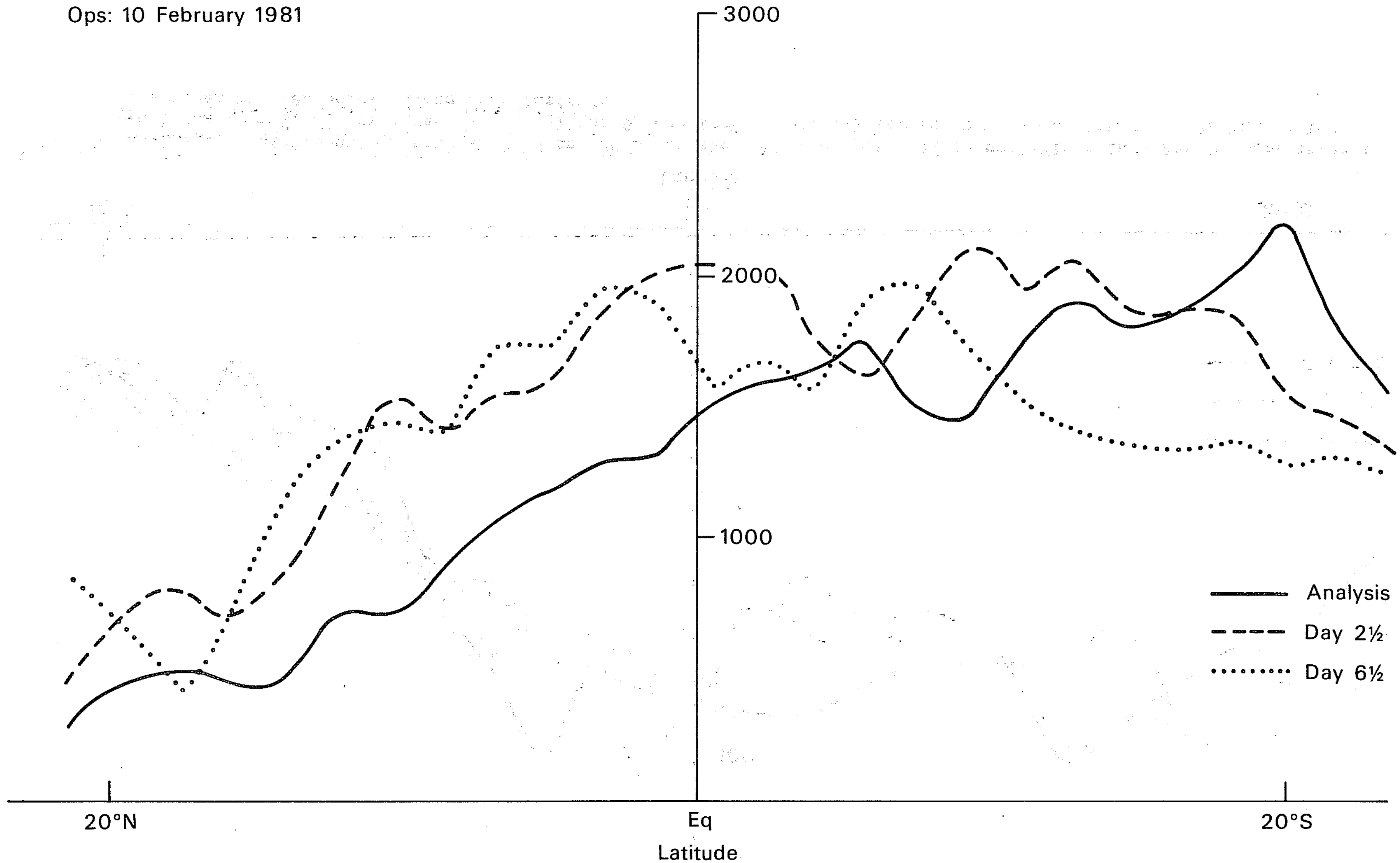

Fig. 24 Latitudinal distribution between 20°N and 20°S, of the zonally averaged values of cloud available potential energy for potentially unstable points. Operational analysis (——), the forecast at day 2½ (----) and the forecast at day 6½ (....) for the operational run on 10 February 1981.

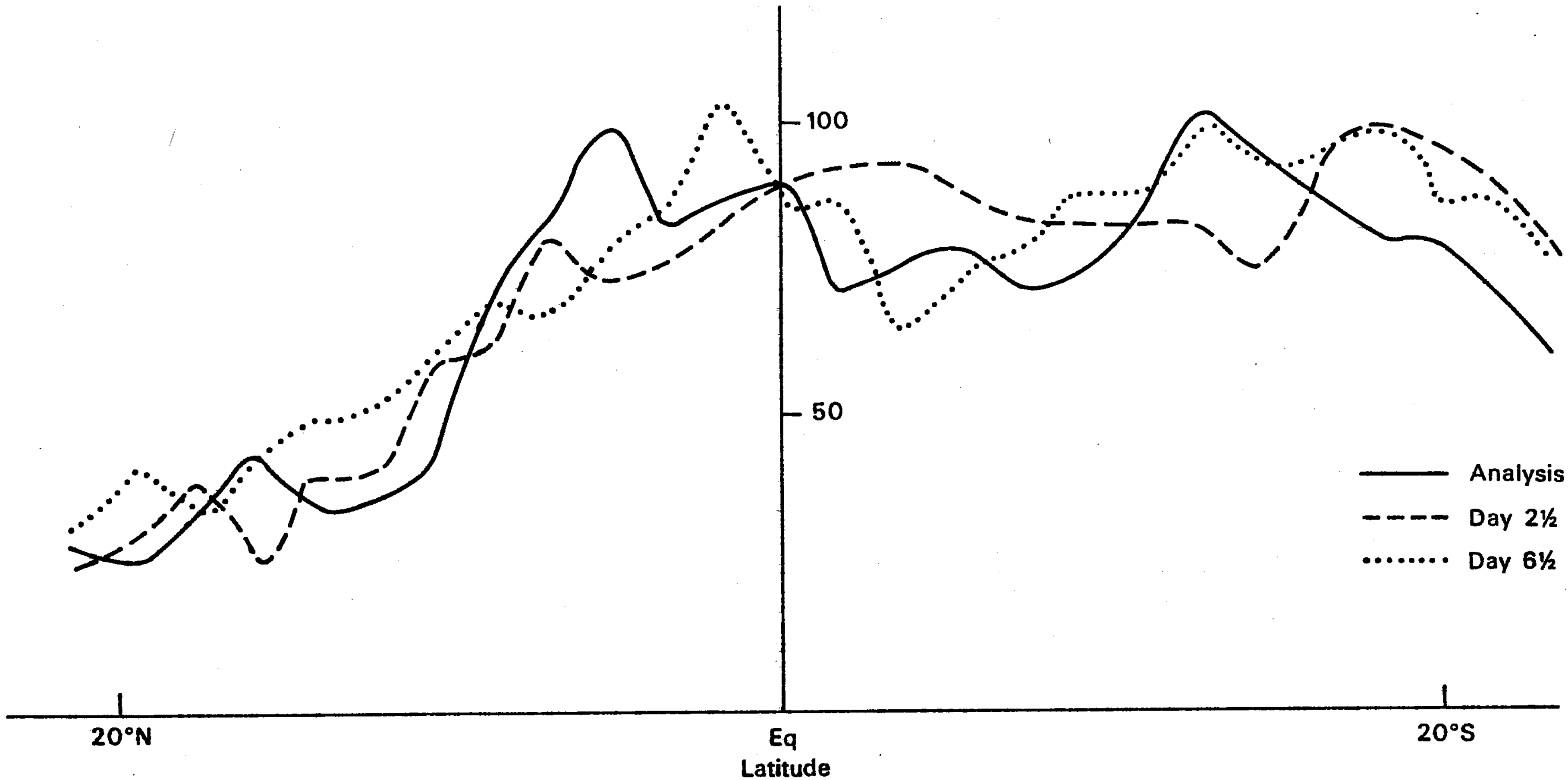

Fig. 25 Latitudinal distribution, between 20^{o}N and 20^{o}S, of the number of potentially unstable points for the operational analysis (——), $2\frac{1}{2}$ day fore-cast (----) and $6\frac{1}{2}$ day forecast (....) for the operational run of 10 February 1981. The model has 192 points along each latitude.

The conclusion from these results is that the present convection scheme as implemented has some peculiar properties. In the mean the model tropics are extremely unstable; the convection scheme releases insufficient precipitation; the trade winds weaken in the first few days of the forecast and then recover presumably due in part to diabatic processes; the convection that does occur seems to generate intense local features too frequently, and towards the end of the forecast there appears to be a tendency to concentrate the tropical convection in a single area.

5. OTHER TESTS

The work presented here indicated little response of the model tropics to a more intense divergence field in the initial data. However there appears to be some aspects of the convection scheme which are unsatisfactory and which may well suppress sensitivity to the initial divergence field. In principle it should be possible to run the assimilation with initialization only one or at most two modes in the vertical. For the moment, given the behaviour of the convection scheme, a reasonable compromise would appear to be the one used here, that of initializing only two modes on the longest scales and five for the smaller scales.

This suggestion still needs further testing on other cases. In a preliminary experiment we considered the situation already discussed in relation to Fig. 8 - an intense convective area over Australia on December 11, 1980. This experiment (called D1) re-ran the assimilation from 12Z on December 10 initialising three modes in the vertical for zonal wavenumber M524 and 5 nodes otherwise. Fig. 26 is directly comparable with Fig. 8 and shows how the uninitialized and initialized vertical velocity field at 6Z together with the forecast field at 12Z on December 11. We see that the change in initialization from Fig. 8 to Fig. 26 has meant a substantial increase in the intensity of the vertical velocity. However at 12Z there was only a minor change in the data rejections in the D1 experiment with one datum at one level from a pilot balloon being rejected in the experiment. To get a feeling for the relative effect of the differences between initialization with three modes and 2 modes we have Fig. 27 which shows the uninitialized data at 12Z together with the initialized vertical velocity from the D1 experiment (3 modes if $k \leqslant 24$, 5 modes otherwise) and initialization with only 2 modes for $k \leqslant 7$ and 5 nodes otherwise. It seems a little surprising that the change in the number of horizontal modes has relatively little effect on this fairly small scale feature. The difference in the number of vertical modes can be seen in the absence of the sinking motion in the stratosphere in Panel c as compared with Panel b.

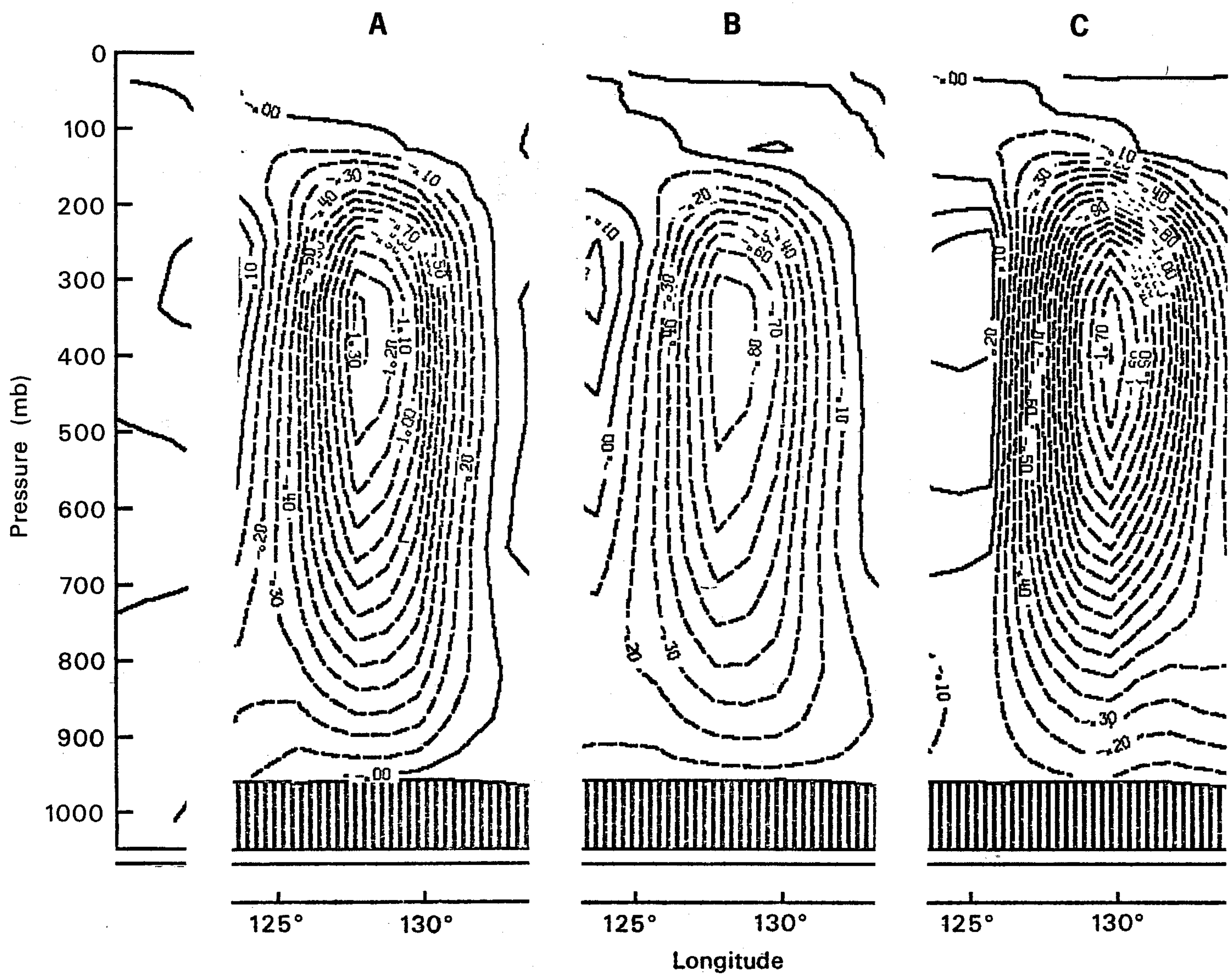

Fig. 26 Cross-sections of the ω-field at $25^{O}S$ between $125^{O}E$ and $135^{O}E$ from an experiment (D1) where we initialised 3 vertical modes for zonal wave number $m \geqslant 24$ and 5 vertical modes, otherwise a) uninitialised analysis, 0600 GMT 11 December 1980 b) initialised analysis 0600 GMT c) 6-hour forecast valid 1200 GMT. The contour interval is 0.1 Pa/s.

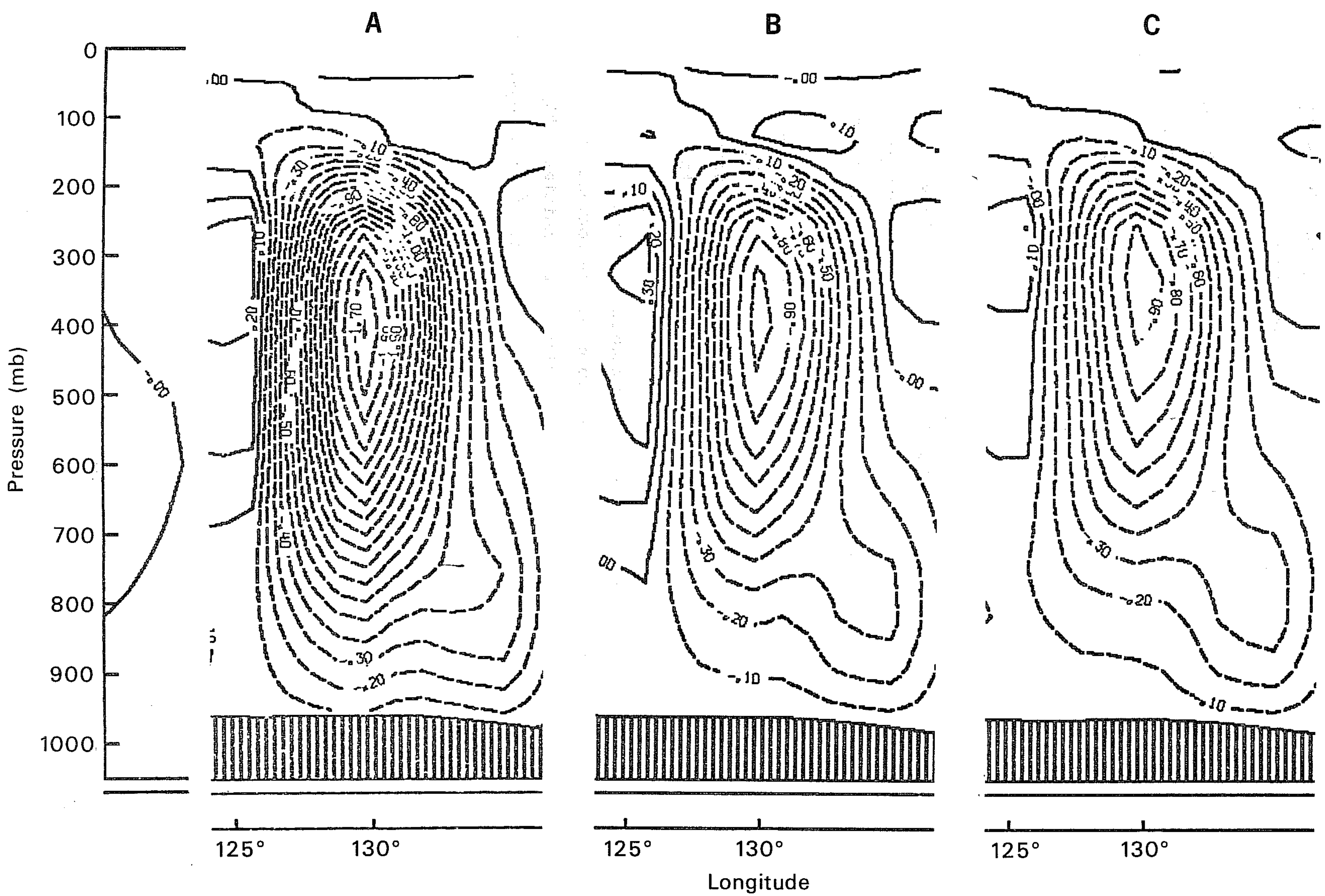

Fig. 27 a) and b) show cross-sections of ω for the uninitialised analysis and initialised analysis at 1200 GMT, 11 December 1980 in the D1 expt. (cf. Fig.26). c) shows the corresponding initialised analysis if we initialise 2 vertical modes for m ⩾7 and 5 modes otherwise.

Neither experiment D1 nor our main experiment indicate any significant problems in running the assimilation with fewer modes being initialized, and they show a desirable increase in the intensity of the tropical circulation.

We may make some comments here on the question of whether one should initialize fewer modes or should include the diabatic forcing in an initialization with many vertical modes. We feel that the latter choice is unwise at the moment given the properties of the convection scheme. The former option appears to achieve the same end and to be more reliable from an operational point of view.

6. SUMMARY AND CONCLUSIONS

It is shown that one can run the ECMWF assimilation system for at least a day while preserving a reasonable intensity of the divergent flow in the tropics by initializing a smaller number of modes. It is particularly important not to initialize vertical modes 3 and 4 on the largest horizontal scales. A test forecast did not exhibit much sensitivity to the more intense divergence fields. This may be because errors in the treatment of tropical atmosphere are so large in the first few days. These errors are shown to occur systematically and to be of large horizontal scale. It is also shown that the convection scheme produces unreasonable values for the cloud available potential energy in the tropics. The two errors are possibly connected. Finally we are of the view that with the present version of the convection scheme it would be unwise to include the diabatic heating in the initialization procedure for the purpose of intensifying the initialized tropical circulations.

REFERENCES

Julian, P. 1980 Data assimilation for the FGGE tropical observing system, in ECMWF Seminar 1980: Data assimilation methods, pp.375-398.

Leith, C.E. 1980 Nonlinear normal mode initialization and quasi-geostrophic theory. J.Atmos.Sci., 37, pp. 958-968

Machenhauer, B. 1977 On the dynamics of gravity oscillations in a shallow water model with applications to nonlinear normal mode initialization. Beitrage zur Physik der Atmosphere, 50, 253-271.

Moncrieff, M. 1981 A theory of organised steady convection and its transport properties. Quart.J.Roy.Meteor.Soc., 107, pp.29-50.

Temperton, C. and D.L. Williamson 1979 Normal mode initialization for a multi-level grid point model. Tech.Report No.11, ECMWF.